NATIONAL ADVISORY COMMITTEE FOR AERONAUTICS

TECHNICAL NOTE 3466

AN INVESTIGATION OF THE DISCHARGE AND DRAG CHARACTERISTICS OF AUXILIARY-AIR OUTLETS DISCHARGING INTO A TRANSONIC STREAM

By Paul E. Dewey and Allen R. Vick

Langley Aeronautical Laboratory
Langley Field, Va.

Washington

July 1955

NATIONAL ADVISORY COMMITTEE FOR AERONAUTICS

TECHNICAL NOTE 3466

AN INVESTIGATION OF THE DISCHARGE AND DRAG CHARACTERISTICS OF AUXILIARY-AIR OUTLETS DISCHARGING INTO A TRANSONIC STREAM

By Paul E. Dewey and Allen R. Vick

SUMMARY

The flow characteristics of a series of rectangular outlets which discharge air into a transonic stream, together with the wall static-pressure distributions in the vicinity of the outlets and the thrust coefficients of rectangular and circular outlets, are presented herein. Discharge coefficients are presented as a function of the discharge flow ratio, defined as the ratio of the measured discharge rate to the rate of flow through a stream tube with a cross-sectional area equal to that of the outlet. Wall static-pressure distributions are shown as pressure coefficients for several values of discharge flow ratio and Mach number. Thrust coefficients are presented as functions of discharge flow ratio at several stream Mach numbers for some of the outlets tested.

Rectangular thin-plate outlets of aspect ratios from 1/10 to 10 were found to have approximately equal discharge coefficients at high flow ratios. At lower discharge rates, the outlets of lower aspect ratio have higher discharge coefficients. Recessed ducted outlets exhibit very high discharge coefficients at low discharge rates. At high discharge rates, these coefficients are approximately the same as those of the flush ducted outlets. Correlation with previously published data for circular thin-plate and inclined outlets is excellent.

The discharge from the inclined ducted outlets produces thrust which approaches the value of the streamwise component of the ideal thrust.

INTRODUCTION

In the design of modern aircraft which operate in the transonic speed range, many factors which were formerly considered as negligible assume such proportions as to affect the performance of the aircraft seriously. Among these are the large numbers of vents, drains, and auxiliary-air outlets which are necessary to the successful operation of such aircraft. The designer of these installations must have reliable data on the force

and discharge characteristics if he is to provide for the most efficient disposal of liquids and auxiliary air.

The present investigation is part of a general research program to determine experimentally the discharge coefficients and the drag or thrust forces of auxiliary-air outlets in the presence of a transonic airstream. References 1 and 2 contain data on discharge characteristics of circular and elliptical outlets discharging into a transonic stream, but the only data available on the force characteristics of outlets are those presented by Rogallo (ref. 3). These data were taken at a maximum tunnel Mach number of approximately 0.1. Data for rectangular outlets, obtained in tests similar to those of references 1 and 2, are presented herein, together with drag (or thrust) characteristics of several outlets as determined from dynamometer measurements. Surface pressures measured in the vicinity of each outlet are also presented for several discharge flow ratios. All testing was done with the outlet models installed in an area of negligible pressure gradient in a region where the boundary-layer thickness was approximately 1/8 inch.

The purpose of this report is to provide the designer with information on the force and discharge characteristics of flush auxiliary-air outlets. The variables considered were aspect ratio, inclination, curvature, and recess depth. Both thin-plate and ducted-approach outlets were investigated over a range of stream Mach numbers from 0.7 to 1.3.

SYMBOLS

A outlet cross-sectional area

C_T thrust coefficient, T/qA

K outlet discharge coefficient, $\dfrac{\text{Measured mass flow}}{\text{Calculated (ideal) mass flow}}$

K_o outlet discharge coefficient in still air, $\dfrac{\text{Measured mass flow}}{\text{Calculated (ideal) mass flow}}$

m outlet discharge mass-flow rate

M tunnel Mach number

P outlet total pressure

p stream static pressure

q	stream dynamic pressure, $\rho V^2/2$
R	Reynolds number based on outlet hydraulic diameter
r	radius of curvature of downstream side of outlet throat
T	thrust
t	outlet-throat width
V	stream velocity
x	distance along tunnel axis, positive downstream
α	angle of inclination measured between outlet axis and tunnel wall, deg
ρ	tunnel-air density
$\frac{m}{\rho VA}$	discharge flow ratio, $\frac{\text{Outlet mass flow}}{\text{Tunnel mass flow through area equal to outlet area}}$
$\frac{\Delta p}{q}$	pressure coefficient, $\frac{\text{Local static pressure - Stream static pressure}}{\text{Stream dynamic pressure}}$

EQUIPMENT

The transonic tunnel in which these tests were conducted has a test section $4\frac{1}{2}$ inches high, $6\frac{1}{4}$ inches wide, and 17 inches long (fig. 1). The upper wall is a solid flat plate with an opening to accommodate the outlet models. Glass side walls permit visual observation of the flow with a schlieren system. The lower wall is slotted longitudinally so that 1/5 of its area is open. Below the slotted wall is a chamber which is connected to a vacuum system by means of which the flow through the slotted wall is regulated to control the test-section Mach number above $M = 0.95$.

The outlet air was supplied through a 2-inch pipe from the tunnel supply duct (fig. 2). The rate of flow was controlled by a valve and measured with a calibrated metering orifice installed in the air line.

Forty-mesh screens were installed upstream of the orifice and the outlet to insure uniform velocity distributions at these points.

Two types of models were employed in the investigation of discharge characteristics (fig. 3). For the thin-plate models, square-edge orifices having width-to-length ratios of 1, 2, 4, 6, and 10 were machined in circular brass inserts. The plate thickness of all these models was 1/16 inch. The square ducted-approach outlets were built of wood and plastic. Their external shape was rectangular, so that the models fitted into a steel shell attached to the outside of the upper wall of the test section (fig. 3(b)). Each of these models had a 1/2-inch-square throat.

The tunnel total pressure was measured at a point upstream of the test section. The stream static pressure was measured at an orifice in the upper wall of the tunnel, $2\frac{1}{2}$ inches upstream of the outlet. These two pressures, combined with the stream total temperature measured in the approach duct, define the stream conditions. The outlet discharge rate was calculated from pressures read at pipe taps in the outlet air line upstream and downstream of the calibrated orifice. Another pressure tap, just above the outlet, measured the outlet total pressure. A row of static-pressure orifices on the center line of the upper wall was used to obtain the surface pressure distribution in the vicinity of the ducted-approach outlets. Surface pressures were recorded photographically from a multiple-tube, mercury-filled manometer. All other pressures were read visually from U-tube manometers.

Force measurements for this investigation were made with the force balance shown in figure 4. This balance is a simple cantilever system consisting of two flat springs attached to a mounting ring at one end, with the other fastened to a barrel which, in turn, contains the outlet. Also attached to the top of the springs is an unbonded strain-gage element which transmits electrically any movement of the barrel to a recorder with an output calibrated in terms of force. Thus for a given mass flow ratio, a continuous record of force against Mach number was obtained. The various outlets used in these force tests were inserted into the barrel of the balance so as to be flush with the tunnel wall. Clearance between the outlet and tunnel wall was kept small (approximately 0.003 inch) and a fouling light was installed to indicate any contact between the two. A drawing of each outlet with pertinent dimensions is shown in the figures with their respective force characteristics. Air for various flow rates was obtained from a tap upstream of the tunnel test section and was piped through a metering orifice to a flexible rubber hose which connected to the barrel of the force balance. The rate of air flow through the outlet was controlled by a manual valve.

RESULTS AND DISCUSSION

Discharge Coefficients

Free jet.- Representative plots of the free-jet coefficients of five of the outlets tested are given in figure 5. For the thin-plate outlets, no effect of Reynolds number was found in these calibrations. For the same Reynolds number values (70,000 to 250,000) an almost negligible Reynolds number effect was found for circular and elliptical thin-plate outlets (ref. 1). In figure 5(a), the coefficients of three of the thin-plate outlets are plotted as functions of the outlet pressure ratio. In this range, the variation of coefficient with pressure ratio is almost linear. As the aspect ratio is increased, the free-jet coefficient first decreases, then increases and becomes nearly constant as the flow through the outlet becomes more nearly two-dimensional.

The free-jet coefficients of two of the ducted-approach outlets are shown in figures 5(b) and 5(c), where lines of constant coefficients are plotted on a grid of Reynolds number against pressure ratio. The K_o values of the 45° inclined outlet range from 0.94 to 0.97 (fig. 5(b)). This range is representative of the values found for most of the ducted-approach outlets, including the curved and recessed models.

The most sharply curved outlet ($r/t = 1$) has much lower values of K_o at low pressure ratios than other ducted models (fig. 5(c)) as a result of flow separation from the small radius of curvature.

Thin-plate outlets.- In the investigation of the discharge characteristics, the thin-plate outlets were tested with the longer sides both parallel and perpendicular to the flow in the stream. This method gave a range of aspect ratios $\left(t^2/A\right)$ from 1/10 to 10. In figure 6, the discharge coefficients of rectangular thin-plate outlets are presented as a function of the discharge flow ratio $m/\rho VA$ on the left side of the figure for outlets with aspect ratios less than 1 and on the right side for aspect ratios higher than 1. Decreasing the aspect ratio below unity results in large increases in K at the lower values of discharge flow ratio. At the higher discharge ratios, the differences in coefficients are smaller. The effect of Mach number is small except for the outlets with the smaller aspect ratios. For these models, the discharge coefficient at low discharge flow rates decreases as the Mach number increases. Data points for five aspect ratios equal to or greater than 1 are plotted, but the curves for only three aspect ratios are shown, because the change in discharge coefficient with aspect ratio is much smaller in this range.

Although the performance of each outlet is shown in figure 6, the effect of the stream upon the coefficient is seen more clearly in figure 7, where the ratio of discharge coefficient to free-jet coefficient

is a function of discharge flow ratio. With increasing $m/\rho VA$, the ratio of the outlet discharge coefficient to the free-jet coefficient increases from 0 to a maximum which at low Mach numbers is greater than unity; the maximum value of K/K_o attained at $M = 1.3$ is on the order of 1.0.

In figure 8, curves of K plotted against $m/\rho VA$ from tests of rectangular thin-plate outlets are compared with those obtained in reference 1 for circular and elliptical thin-plate outlets of the same aspect ratio. The shape of the curves is similar, but the circular and elliptical outlets reach somewhat higher discharge coefficients although the free-jet coefficients of the latter (shown in ref. 1) were 1 to 3 percent lower.

Inclined outlets.- The discharge characteristics of square ducted-approach outlets with various angles of inclination are shown in figure 9. The change in discharge coefficient with inclination is very small. At high values of $m/\rho VA$ the discharge coefficients of the four outlets are about equal. At low discharge rates, the K values are spread somewhat, those outlets which are inclined so as to discharge more nearly parallel to the stream having higher coefficients than those which discharge more nearly perpendicular to the stream. The variations of K/K_o for inclined outlets (fig. 10) are very similar to the variations of K since the values of K_o are high and nearly constant for these outlets.

References 1 and 2 present the same type of data for inclined outlets of circular cross section. Circular and square outlets with inclinations of 30° and 90° are compared in figure 11. There is no significant difference between the discharge characteristics of the square and circular models, although in some cases the coefficients of the circular models are slightly higher than those of the square models.

Curved outlets.- Discharge coefficients of square outlets with curved axes are plotted in figure 12. The radius of curvature of the downstream side, which varied between 1 and 4 times the outlet width, had no effect upon the value of the discharge coefficient, the values of K falling between those of the 30° and the 45° inclined outlets.

The curves of K/K_o plotted against $m/\rho VA$ of the three outlets with the larger radii of curvature are also coincident (fig. 13), but K/K_o for the outlet with the smallest radius of curvature falls well above the other three, and at the higher values of $m/\rho VA$ it reaches values above 1.0 at all Mach numbers as a result of the low free-jet coefficients of this outlet. The flow separation from the small radius of curvature in the free-jet tests appears to be eliminated by the external stream, so that the discharge coefficient increases to values higher than the free-jet coefficient at the same Reynolds number and pressure ratio.

The 60° inclined outlet was modified by rounding the downstream corner; three radii were used to produce values of r/t of 1/2, 1, and 2. The discharge coefficient increases slightly as the radius is increased (fig. 14). Higher values of K were obtained with the largest radius which extended into the throat and provided diffusion at the exit. The K/K_o values are nearly equal, however, because the diffusing section increases K_o as well as K (fig. 15).

The straight 60° inclined outlet, the 60° inclined outlet with $r/t = 1$, and the curved outlet with $r/t = 1$ are compared in figure 16. The modified inclined outlet and the curved outlet are similar in both the radius of curvature of the downstream side and the angle at the intersection of the upstream side and the tunnel wall. The discharge coefficient of the modified inclined outlet falls about midway between those of the straight inclined outlet and the curved outlet; however, the differences are very small.

The most notable point demonstrated by the data presented for flush ducted outlets is the similarity of discharge characteristics. In figure 17 the shaded areas represent the total spread of K for the eleven models tested. For most applications, none of these types demonstrates any real superiority, percentagewise, except at low discharge rates. This figure also shows that there is no significant change in K with changing Mach number in the range covered by these tests.

Recessed outlets.- The recessed outlets (fig. 18) exhibit somewhat different characteristics from the flush outlets. At the higher values of $m/\rho VA$, the discharge coefficient is approximately equal to the free-jet coefficient for all the recessed models tested. As $m/\rho VA$ is reduced, K for the more deeply recessed models stays at this value until $m/\rho VA$ is between 0.3 and 0.5. Below this point, K increases rapidly to such size that it is meaningless, the measured mass flow ratio exceeding the calculated flow by many times as a result of the increasing difference between the exit static pressure and the ambient pressure. For the shallower recessed outlets, K has about the same magnitude as for the flush outlets when $m/\rho VA$ is above 0.4. As $m/\rho VA$ is reduced below this value, the variation in K tends to break in the same manner as it did for the more deeply recessed outlets.

Because K_o is high for these outlets, the curves for K/K_o (fig. 19) are very similar to those for K. The shallower recessed outlet with the smallest radius of curvature has high K/K_o values for the same reason as previously explained for the flush outlet with small radius of curvature.

Surface Pressure Distribution

Static-pressure readings were taken from the orifices installed in the tunnel wall on a longitudinal line through the center of the inclined, curved, and recessed outlets. These data have been reduced to a pressure coefficient and plotted against axial distance at three Mach numbers for three values of the discharge flow ratio (fig. 20). The surface pressures with no discharge from the outlets are also shown by the circular symbols. The point $x = 0$ was not taken from a static-pressure orifice in the tunnel wall but was read from the outlet total-pressure tube.

These pressure distributions for the flush outlets all show the same general characteristics. As the outlet is approached from the upstream side, the pressure rises; the strength and extent of the disturbance increases as the discharge rate is increased. This rise is more abrupt at supersonic Mach numbers because of the shock wave which stands ahead of the outlet. It is smaller for the more inclined and curved outlets which discharge in a direction more nearly parallel to the stream. Immediately downstream of the outlet, the pressure is far below the free-stream static pressure. Continuing downstream, the pressure rises until it reaches the free-stream value at a distance of about 8 throat widths from the outlet.

The pattern of surface pressure near the shallow recessed outlets resembles that for the flush outlets. The discharge from the deeper recessed outlets causes no disturbance upstream and only a small variation in pressure downstream.

Vent Pressures

In an application in which an auxiliary-air outlet is intended for intermittent operation, the pressure in the space exhausted by the outlet may be an important factor from the standpoint of drag or for structural reasons. These vent pressures are presented in the form of pressure coefficients as functions of Mach number (fig. 21) for several of the outlets tested. In the thin-plate outlets, the pressure with no flow varied little from that in the stream. In the inclined outlets, the vent pressures were very slightly lower than the stream static pressure. The recessed outlets have vent pressures which are below the stream static pressure by from 10 percent to 20 percent of the stream dynamic pressure, the increment increasing with Mach number. This low pressure which represents the base pressure across the outlet will result in high drag at the no-flow condition. The small rise in vent pressure at $M = 1.1$ for some of the outlets is unexplained.

Thrust Coefficients

Several of the flush-type outlets for which flow coefficients are presented in this and an earlier report (ref. 2) have been mounted in a force dynamometer to determine the resultant force in the streamwise direction over a range of mass flow ratios and stream Mach numbers. In figure 22, the ideal thrust coefficient shown as a function of mass flow ratio was calculated from the following equation (subscript e denotes outlet conditions):

$$C_T = \frac{T}{qA} = \frac{mV_e}{qA} = 2\,\frac{m}{\rho VA}\,\frac{V_e}{V}$$

In this equation, the air is assumed to be turned rearward with 100-percent efficiency and discharged from a sonic nozzle at ambient static pressure or, in the case of the choked exit, at $M_e = 1.0$. The experimental results which do not include 100-percent turning of the discharge air make it necessary to include the cosine of the discharge angle when experimental and ideal curves are compared. In presenting the data, the no-discharge-flow force measurements have been subtracted from those obtained with flow and the resulting thrust is presented as a function of the mass flow ratio. These values of thrust coefficient are slightly low because of the change in pressure differential in the small clearance gap (0.005 inch) circumscribing each of the outlets, which increases the tare drag as the discharge flow ratio is increased. The maximum error in C_T amounts to approximately 0.05.

The thrust characteristics of a 1/4-inch-diameter ducted outlet with several different angles of inclination measured from a surface parallel to the airstream are presented in figure 23 as a function of mass flow ratio for Mach numbers of 0.4, 0.7, 1.0, and 1.3. Data for a 60° inclined outlet (fig. 23(a)) show significant values of thrust coefficient for all Mach numbers. These curves drawn for a constant Mach number show an increase in thrust coefficient with an increase in exit flow ratio $m/\rho VA$. For a given mass flow ratio, the highest thrust coefficients occur at the lowest Mach number and decrease with increasing speed. This is contrary to the theory, which indicates only a small Mach number effect prior to choking of the exit. Experimental values show an approximate 40-percent decrease in thrust coefficient at the highest mass flow ratios as the Mach number is increased from 0.4 to 1.3. Figures 23(b) and 23(c) show results for 45° and 30° angles of inclination, respectively. As the inclined angle decreases toward 0°, the thrust coefficient continues to become larger as a greater degree of internal turning is realized. A comparison of the experimental thrust coefficients with those calculated by using the cosine of the discharge angle shows that, for discharge angles of 30°, fair approximations may be made by using the cosine value.

However, as the outlet angle of inclination is increased, the experimental values of C_T are greater than the ideal, the difference decreasing with increasing Mach number or mass flow ratio, or both. The force characteristics for all these outlets were measured in a tunnel in which the boundary layer was approximately 1/8 inch thick. A repeat test of the 60° inclined outlet with the boundary-layer thickness more than doubled showed no significant changes in the thrust characteristics.

In order to determine the effect of changing from a round outlet to a square ducted model, a test was made with the 60° inclined model cut to a square. The results presented in figure 24, when compared with data from tests of the 1/4-inch-diameter outlet (fig. 23(a)), show negligible difference in thrust coefficient due to hole shape.

It is of interest to note that data taken but not presented on the force characteristics of flush thin-plate models and also a ducted-approach model in which the air was discharged perpendicular to the free stream indicated thrust coefficients on the order of 0.2 for mass flow ratios above 0.5. The thrust produced by the thin-plate models is believed to be related to a slight pressure differential that exists on the opposite walls of the duct that contains the outlet. Although the magnitude of the thrust produced by these thin-plate models was small, it is worthwhile noting that a net thrust was produced at all mass flow ratios rather than a drag force.

For those configurations tested, the difference in drag between a plate containing an outlet with no discharge and a solid plate was within ±0.1 ounce.

CONCLUSIONS

As a result of this investigation of aerodynamic characteristics of auxiliary-air outlets the following conclusions may be drawn:

1. The discharge coefficients of rectangular thin-plate outlets which are discharging air into a transonic stream decrease with increasing aspect ratio.

2. Variation of the stream Mach number has no significant effect on the discharge coefficient of any of the flush ducted outlets tested.

3. The recessed outlets tested have high discharge coefficients due to the pumping effect of the stream, especially at low outlet pressures.

4. The variation in surface pressure caused by the outlet discharge decreases as the outlet is inclined or curved to discharge more nearly parallel to the stream; there is almost no disturbance in the stream when the more deeply recessed outlets are discharging.

5. The vent (or duct) pressures at zero discharge flow ratio for all flush outlets are nearly equal to the local stream static pressures. Those of recessed outlets are below the local stream static pressure by from 10 percent to 20 percent of the stream dynamic pressure.

6. The discharge from inclined outlets produces a thrust which very nearly approximates the streamwise component of the calculated ideal thrust.

Langley Aeronautical Laboratory,
National Advisory Committee for Aeronautics,
Langley Field, Va., March 10, 1955.

REFERENCES

1. Nelson, William J., and Dewey, Paul E.: A Transonic Investigation of the Aerodynamic Characteristics of Plate- and Bell-Type Outlets for Auxiliary Air. NACA RM L52H20, 1952.

2. Dewey, Paul E.: A Preliminary Investigation of Aerodynamic Characteristics of Small Inclined Air Outlets at Transonic Mach Numbers. NACA TN 3442, 1955. (Supersedes NACA RM L53C10.)

3. Rogallo, F. M.: Internal-Flow Systems for Aircraft. NACA Rep. 713, 1941.

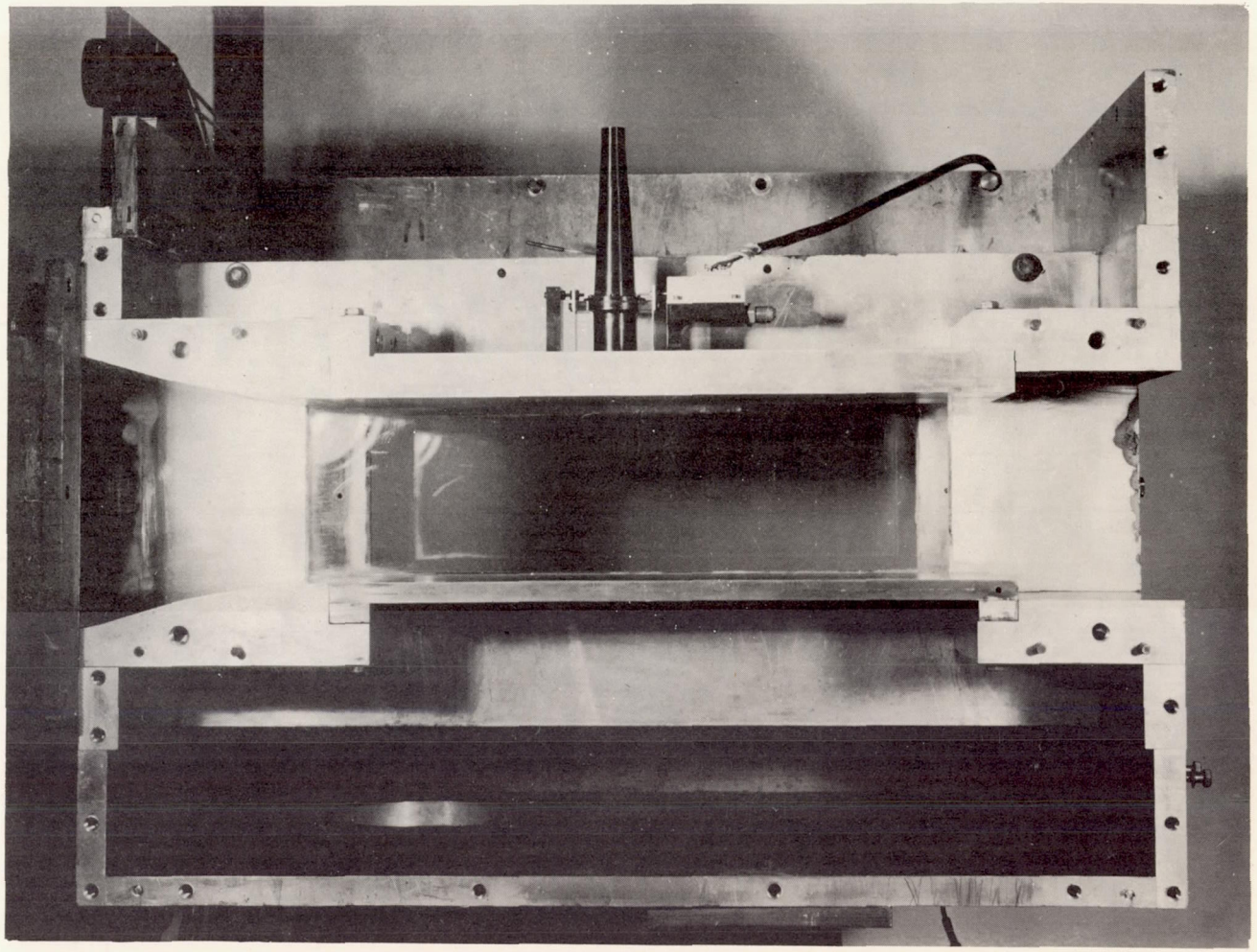

L-82975

Figure 1.- The $4\frac{1}{2}$-inch by $6\frac{1}{4}$-inch transonic tunnel with force balance in position.

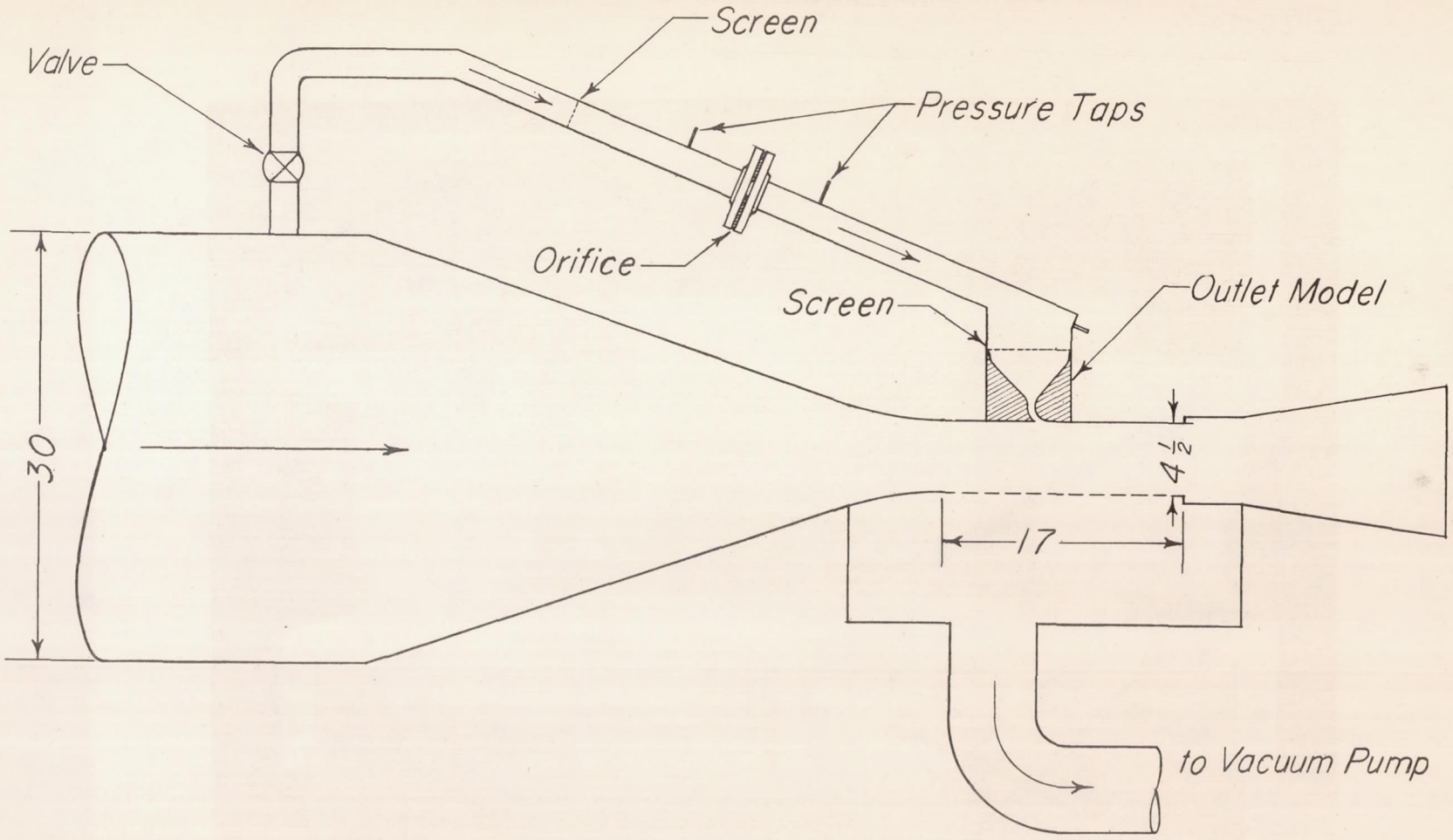

Figure 2.- General arrangement of test setup with ducted-outlet model installed. All dimensions are in inches.

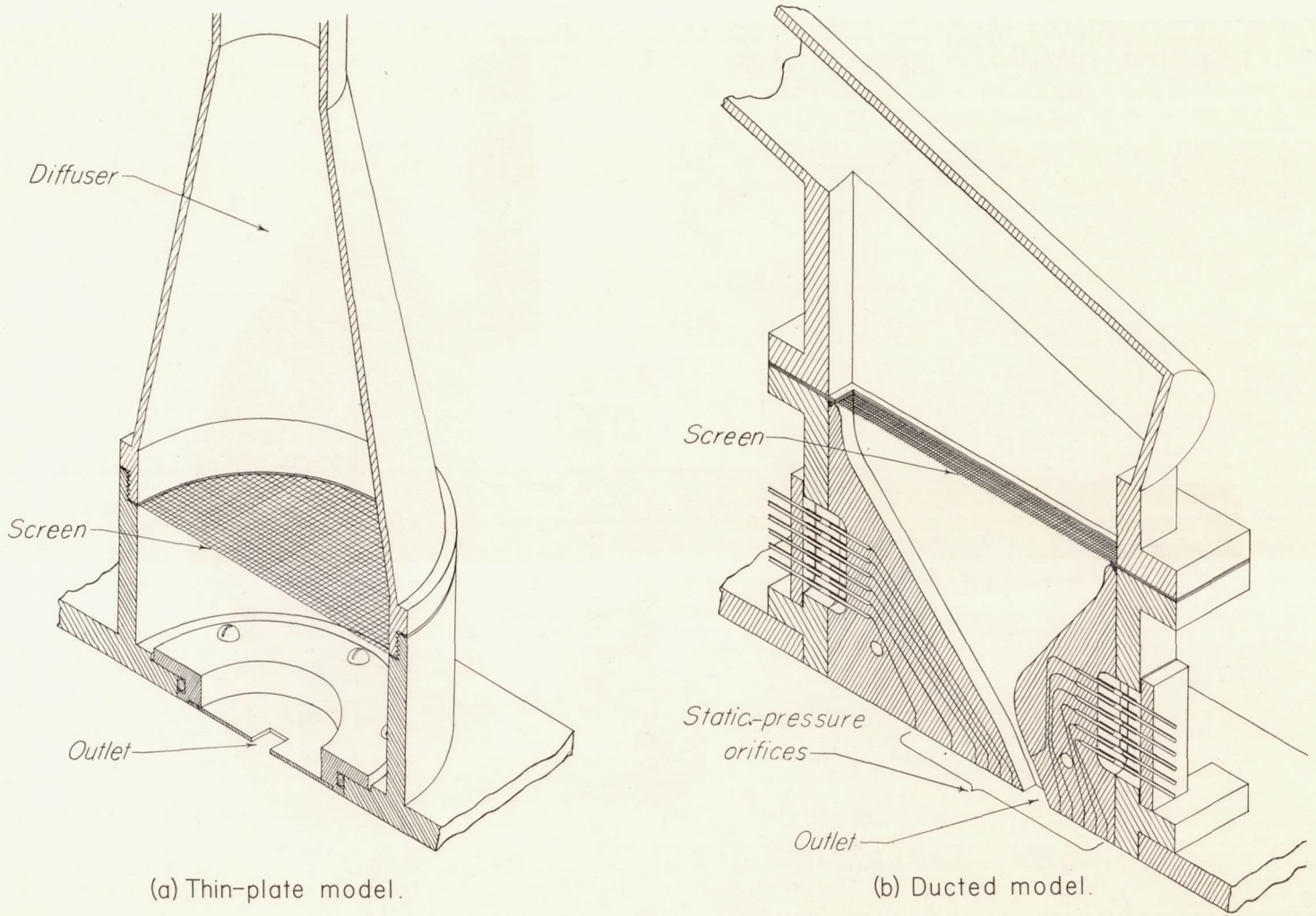

(a) Thin-plate model.

(b) Ducted model.

Figure 3.- Details of outlet installation.

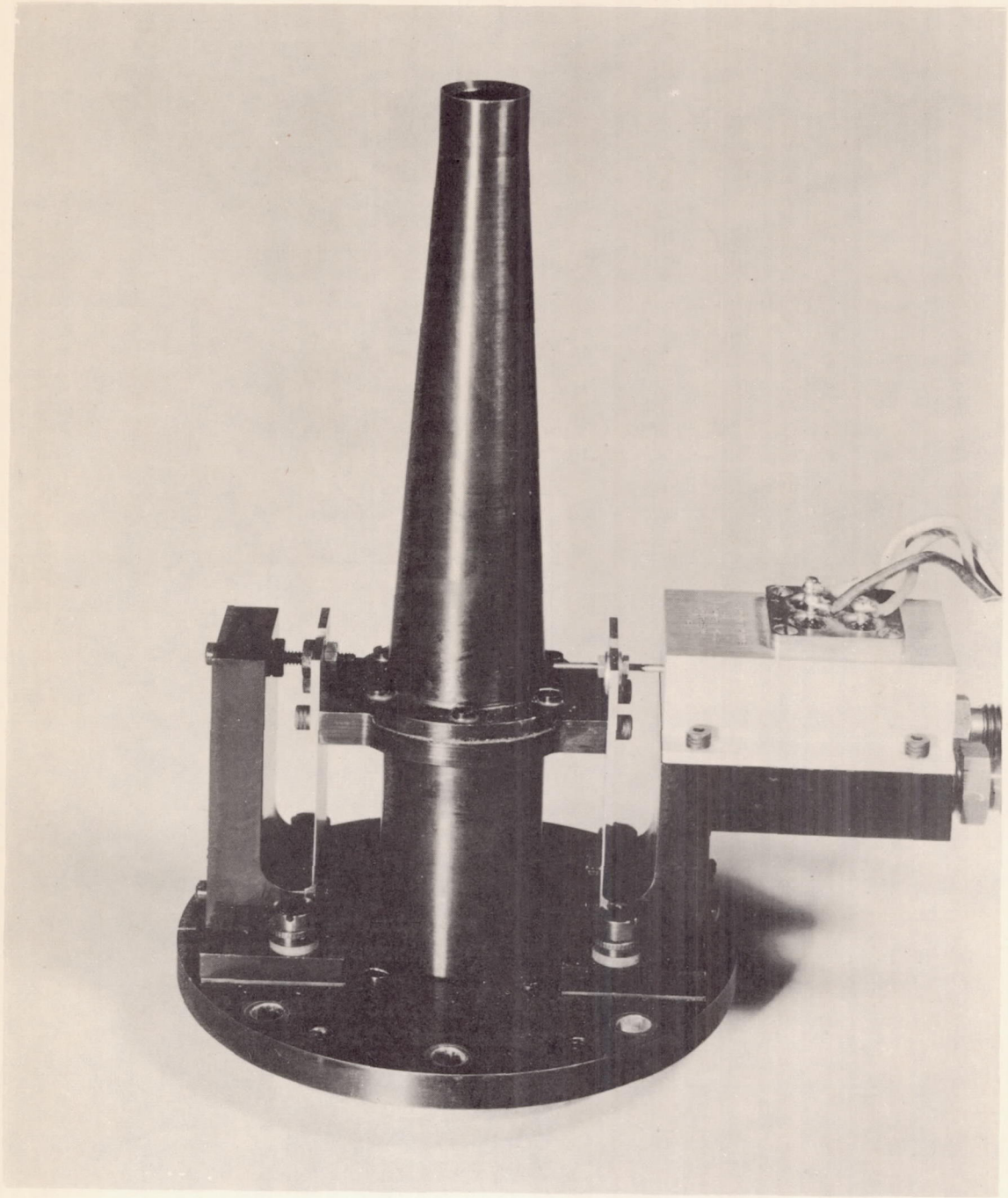

L-82974

Figure 4.- Balance and approach duct used for force measurements.

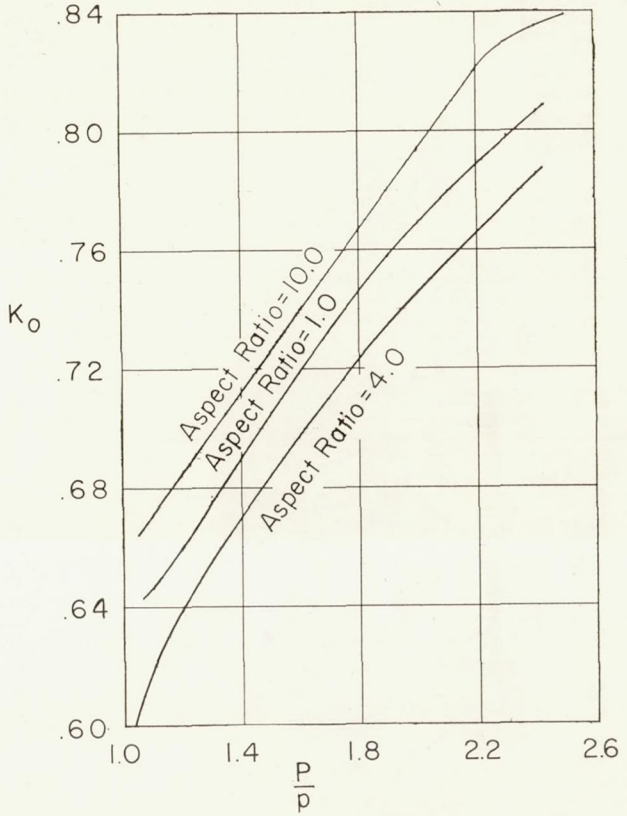

(a) Thin-plate Outlets.

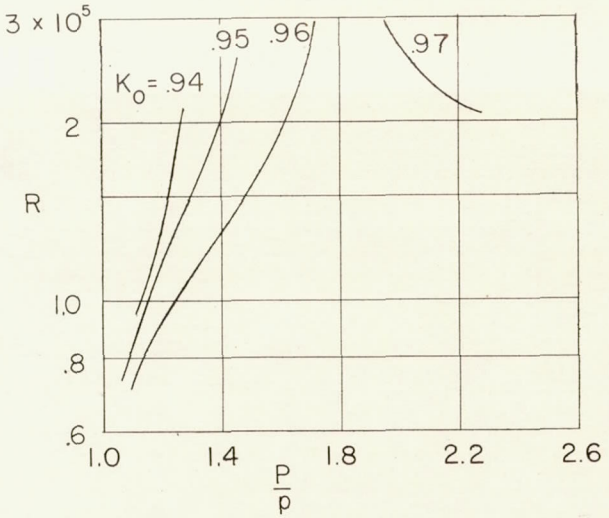

(b) 45° Inclined Outlet.

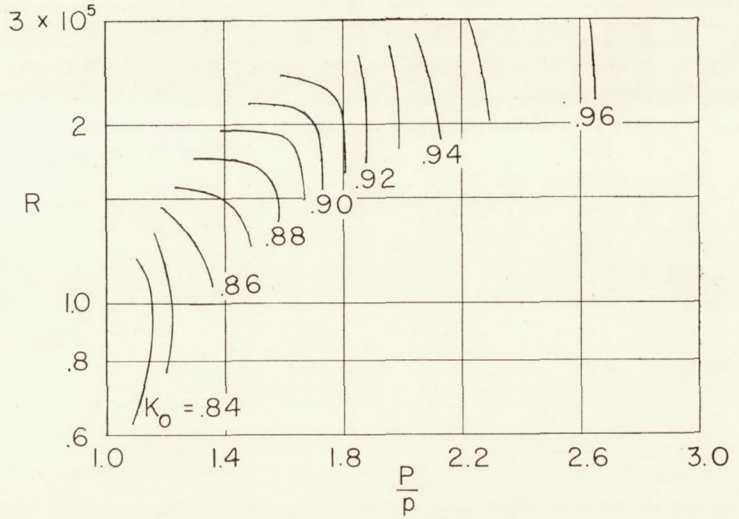

(c) Curved Outlet, $\frac{r}{t}$ =1.0.

Figure 5.- Free-jet coefficients.

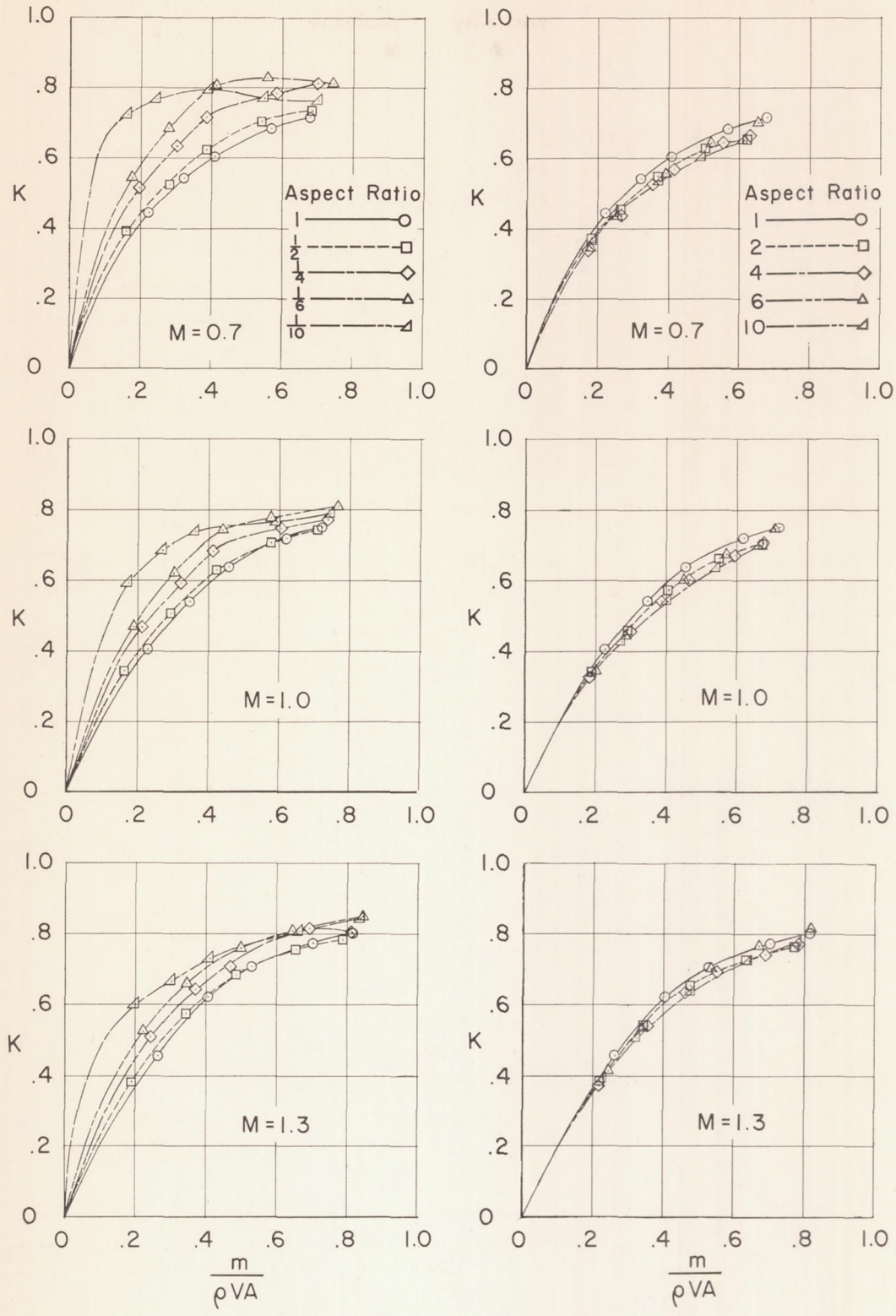

Figure 6.- Discharge coefficient as a function of discharge flow ratio for thin-plate outlets.

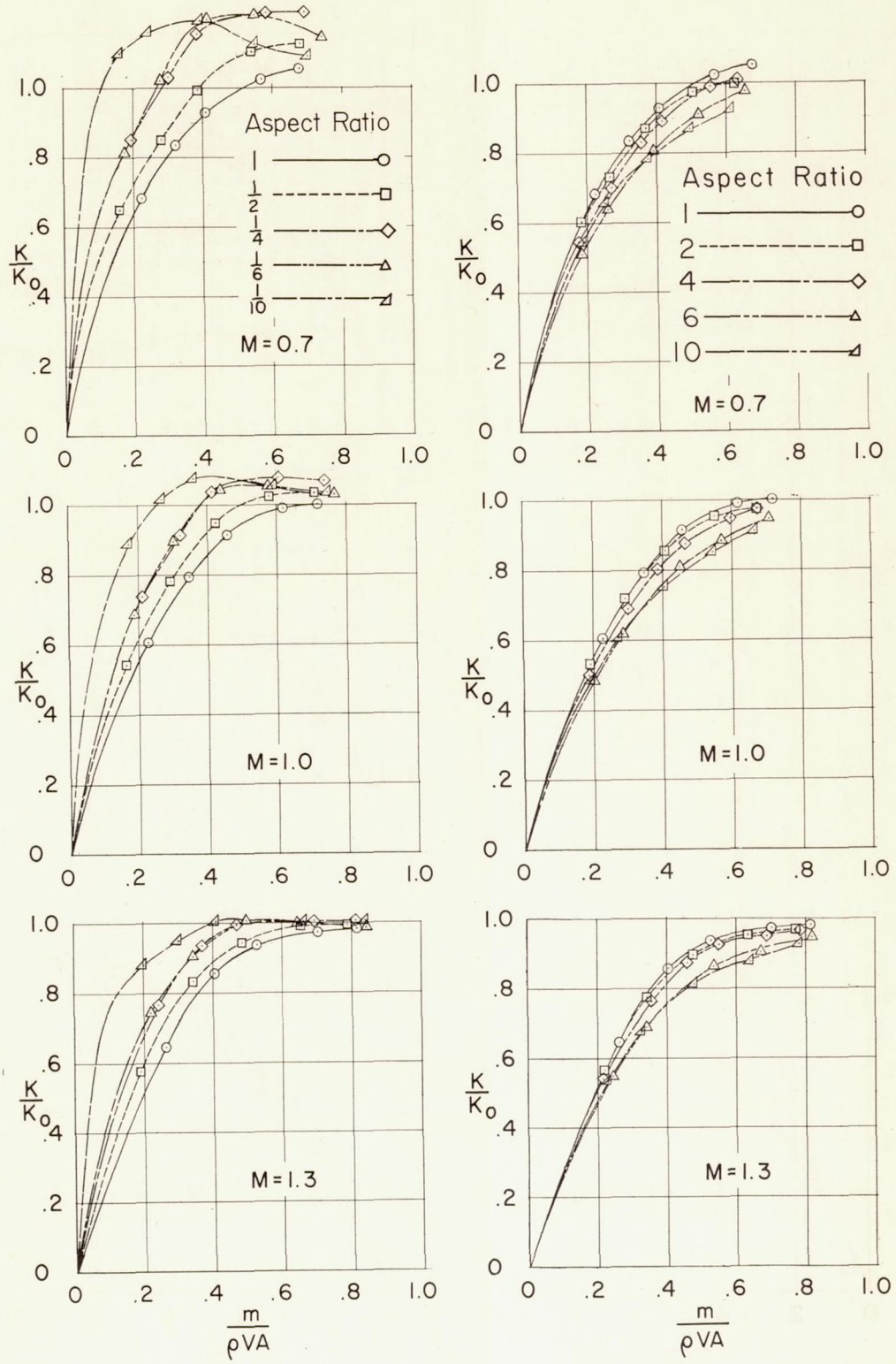

Figure 7.- Ratio of discharge coefficient to free-jet coefficient as a function of discharge flow ratio for thin-plate outlets.

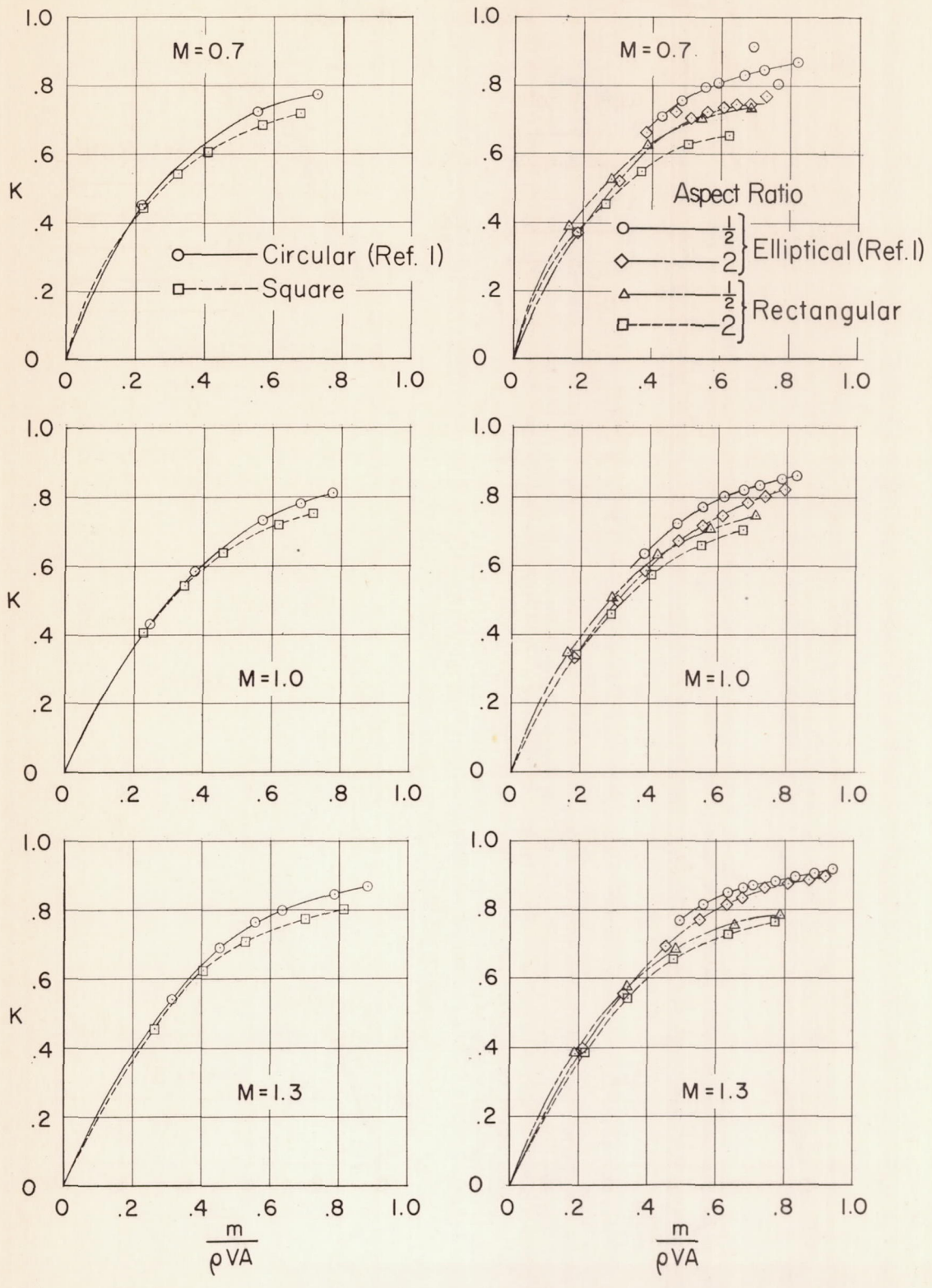

Figure 8.- Comparison of discharge coefficients of rectangular thin-plate outlets with those of circular and elliptical models of the same aspect ratio.

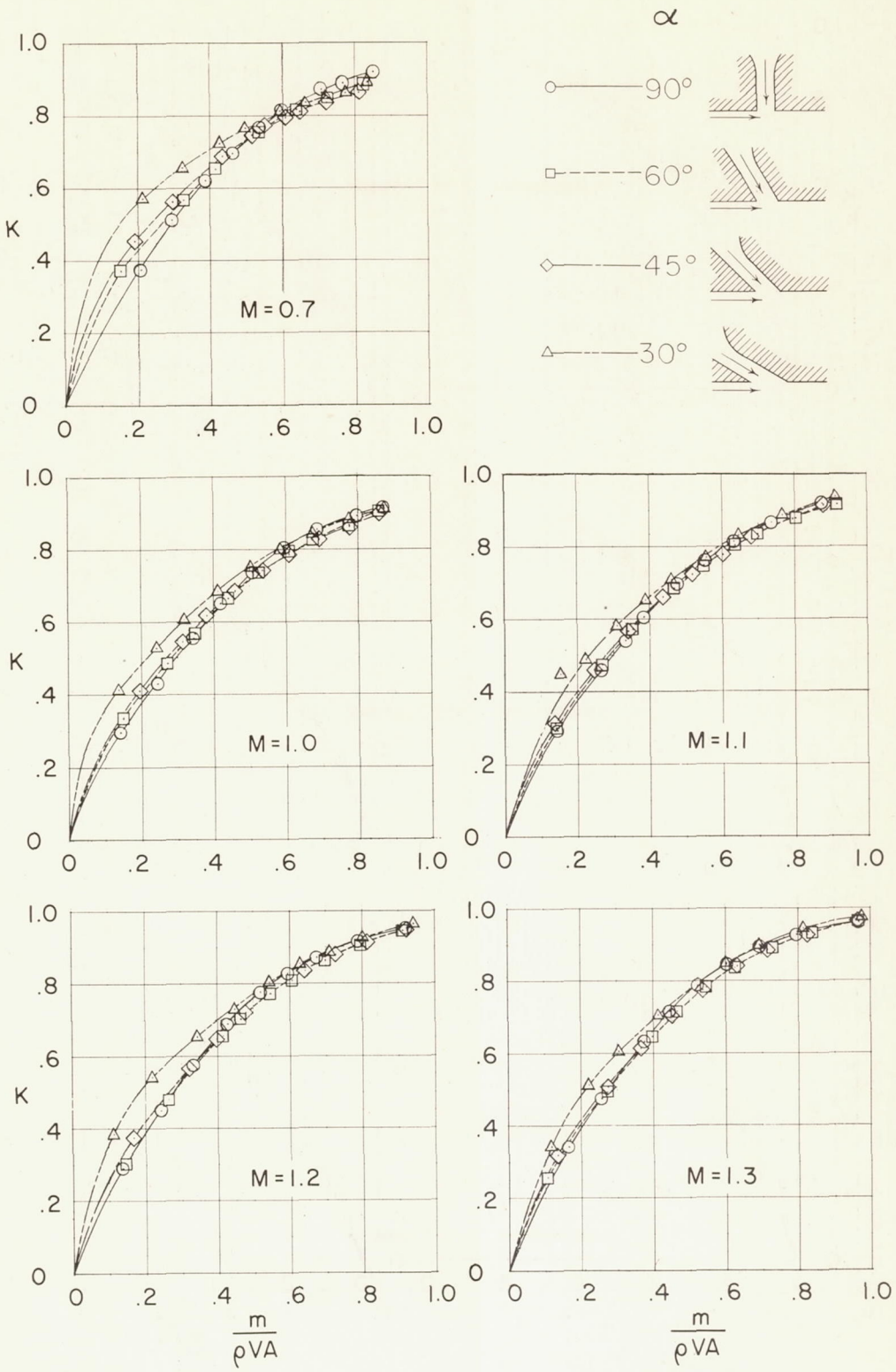

Figure 9.- Discharge coefficient as a function of discharge flow ratio for inclined outlets.

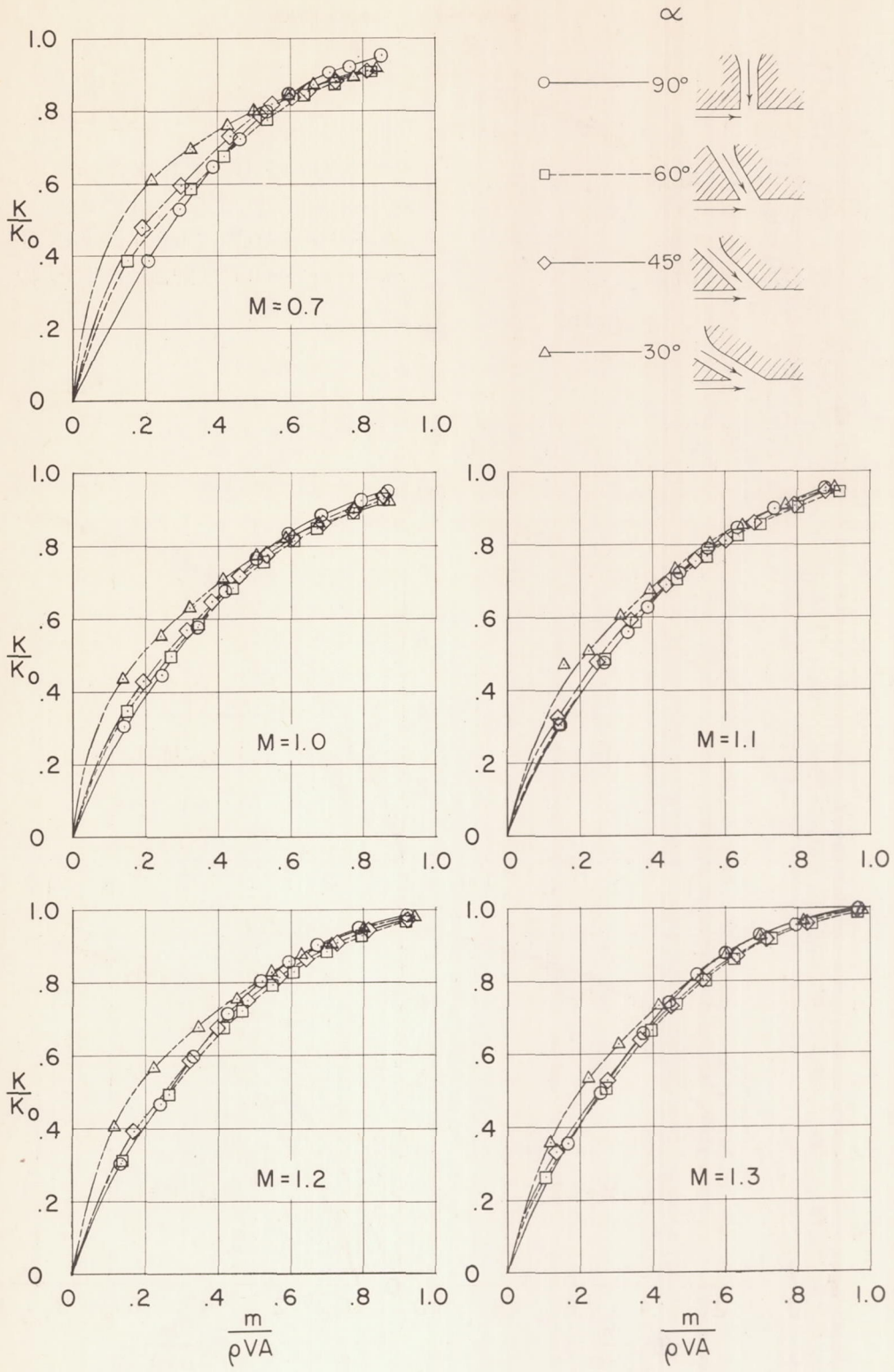

Figure 10.- Ratio of discharge coefficient to free-jet coefficient as a function of discharge flow ratio for inclined outlets.

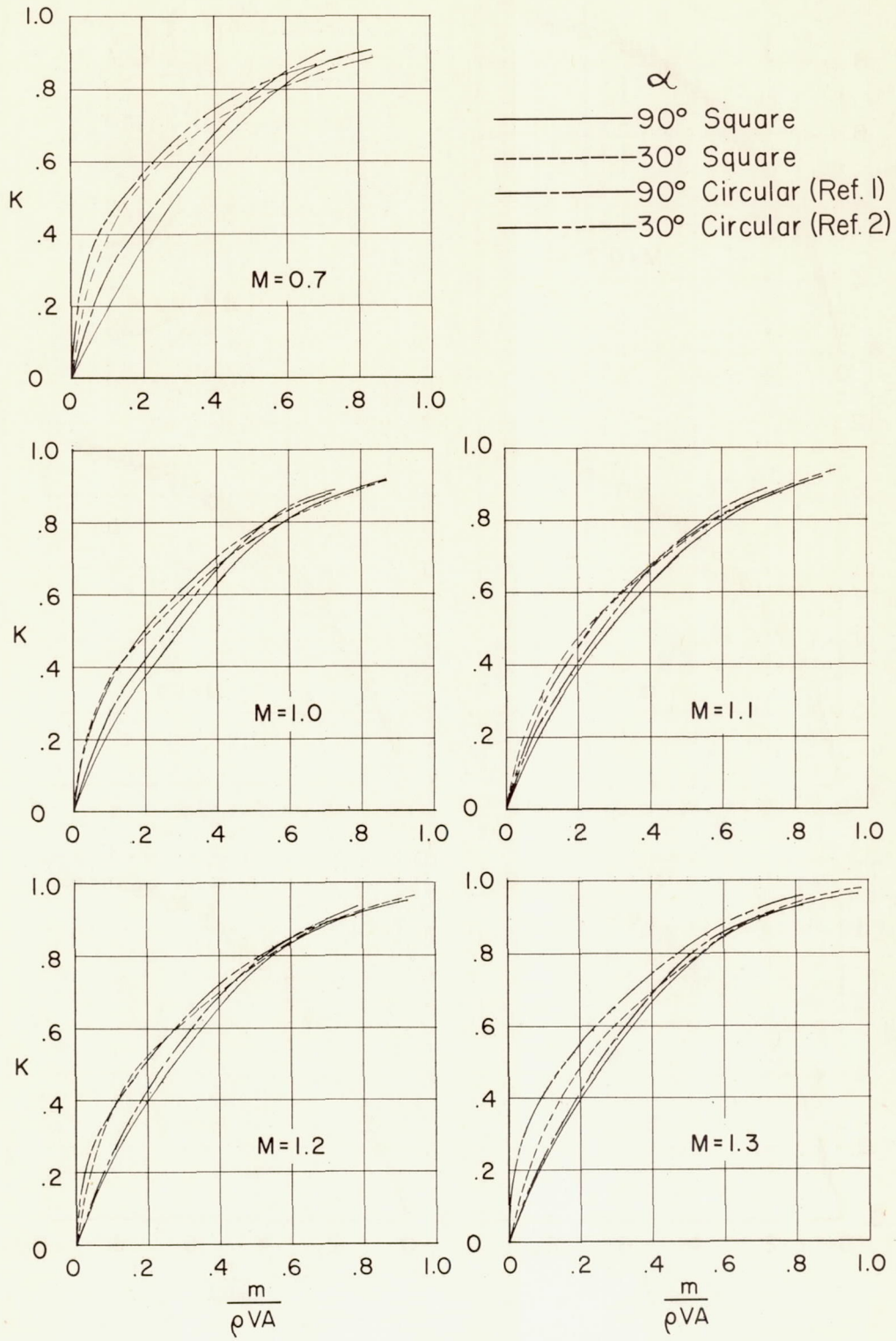

Figure 11.- Comparison of discharge coefficients of square and circular inclined outlets.

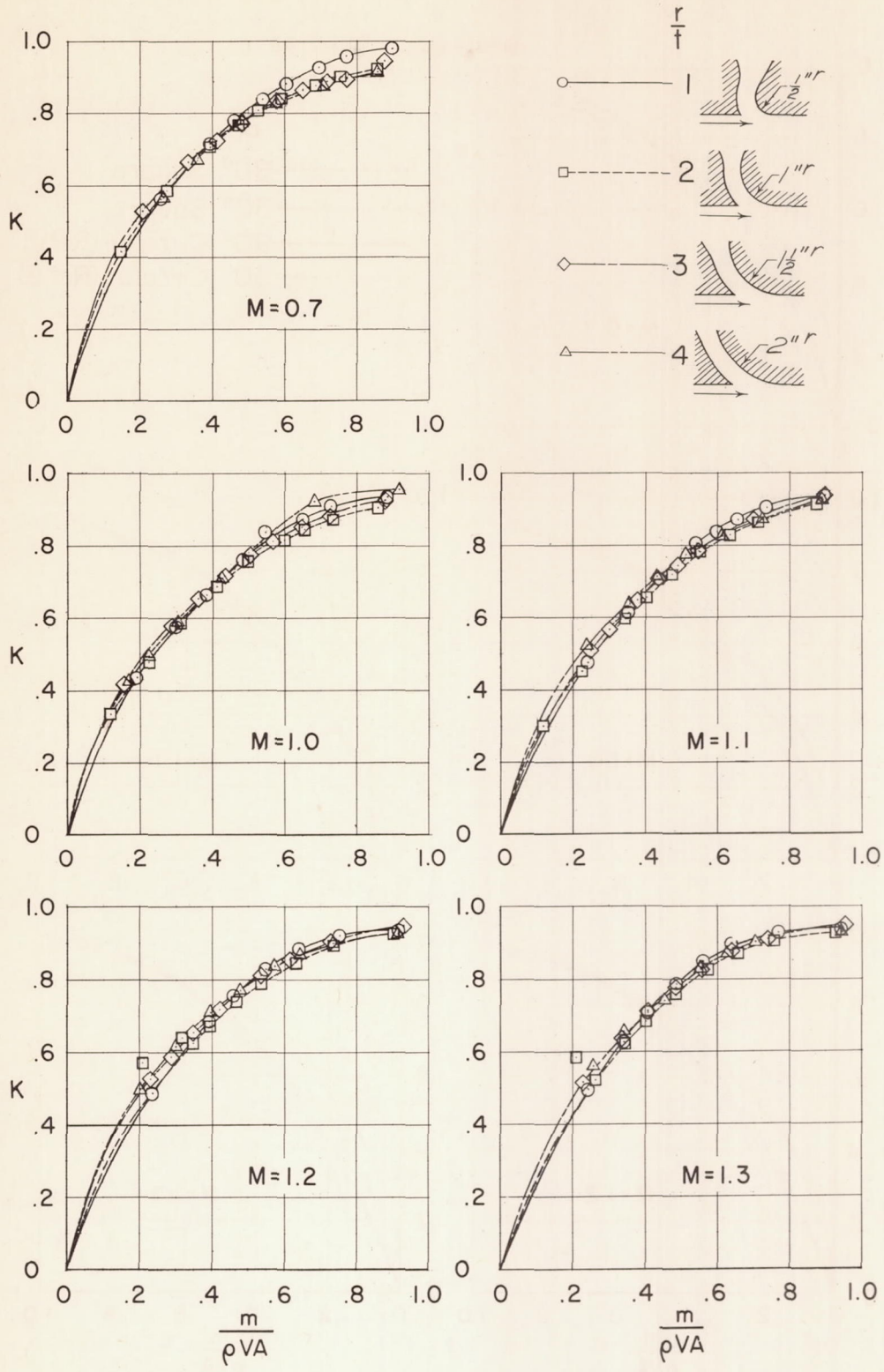

Figure 12.- Discharge coefficient as a function of discharge flow ratio for curved outlets.

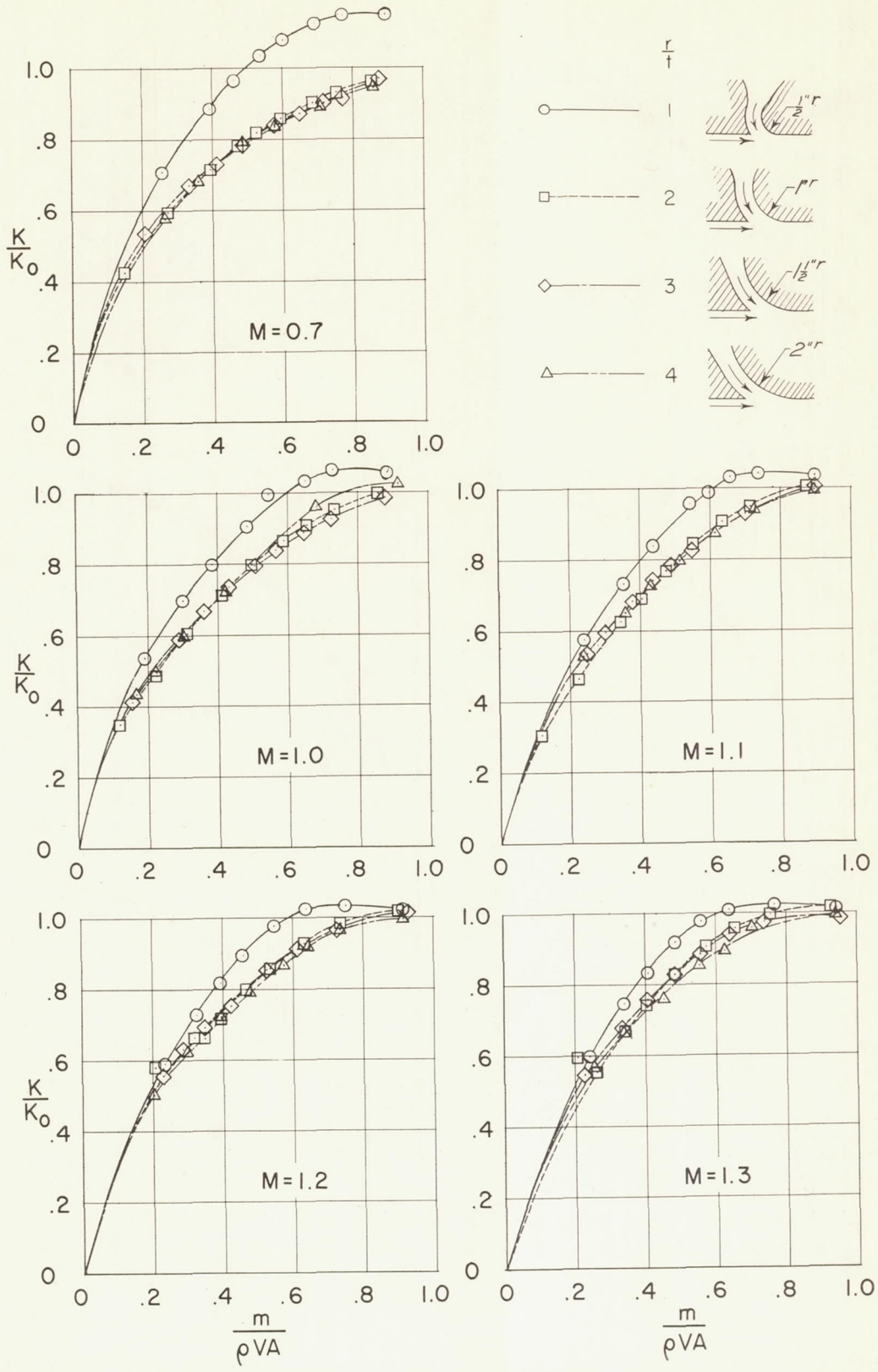

Figure 13.- Ratio of discharge coefficient to free-jet coefficient as a function of discharge flow ratio for curved outlets.

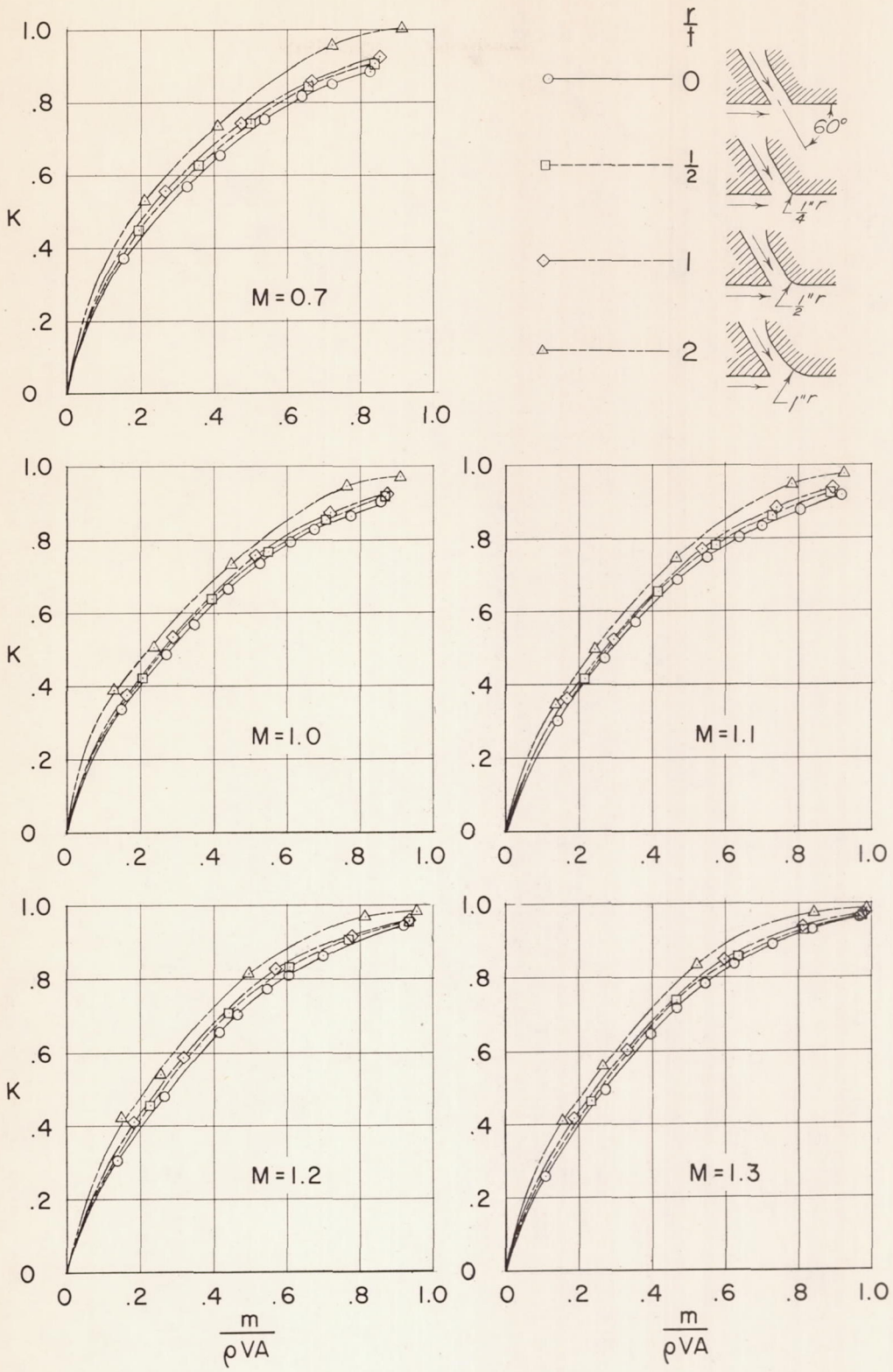

Figure 14.- Discharge coefficient as a function of discharge flow ratio for 60° inclined outlets with various radii at trailing edge.

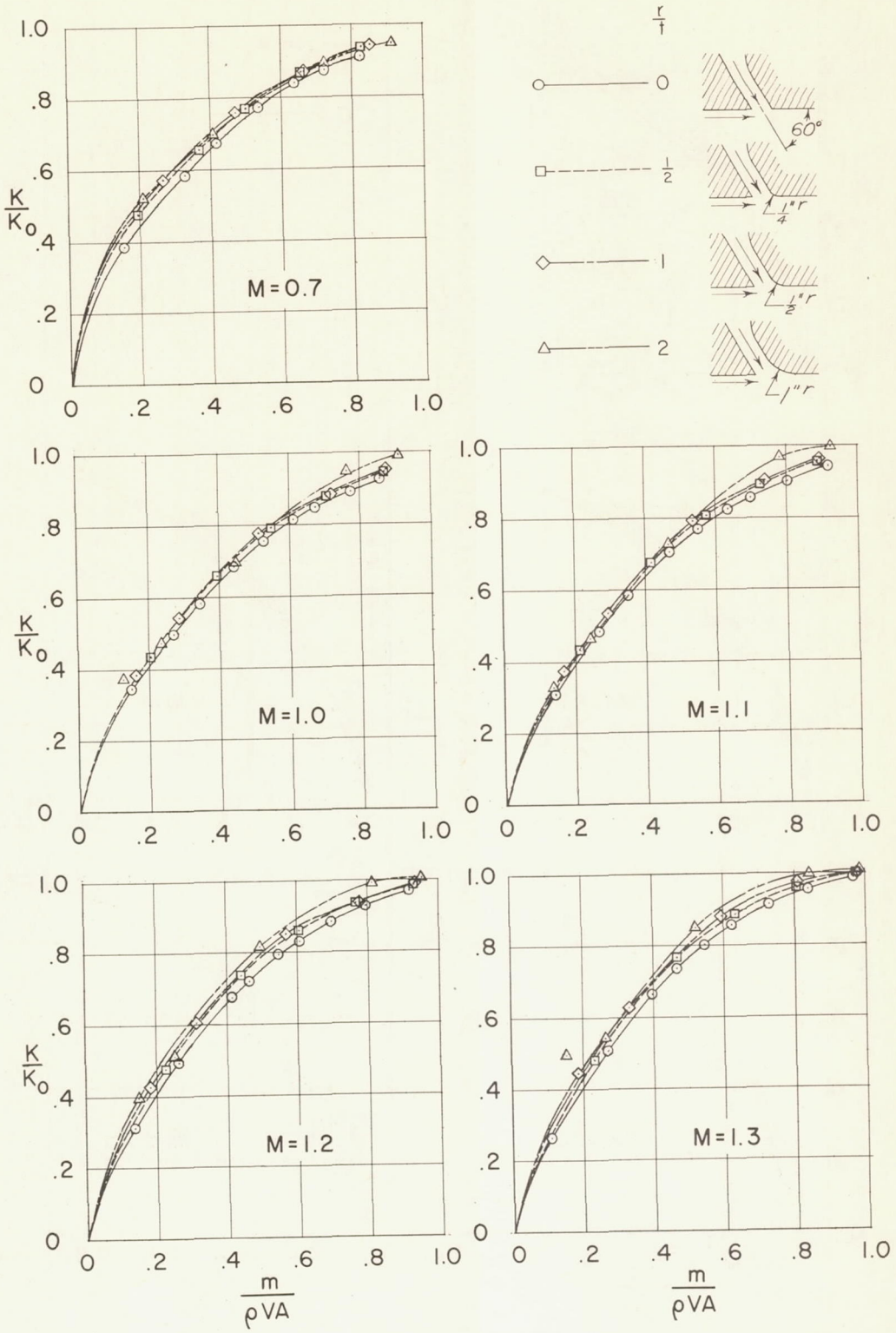

Figure 15.- Ratio of discharge coefficient to free-jet coefficient as a function of discharge flow ratio for 60° inclined outlets with various radii at trailing edge.

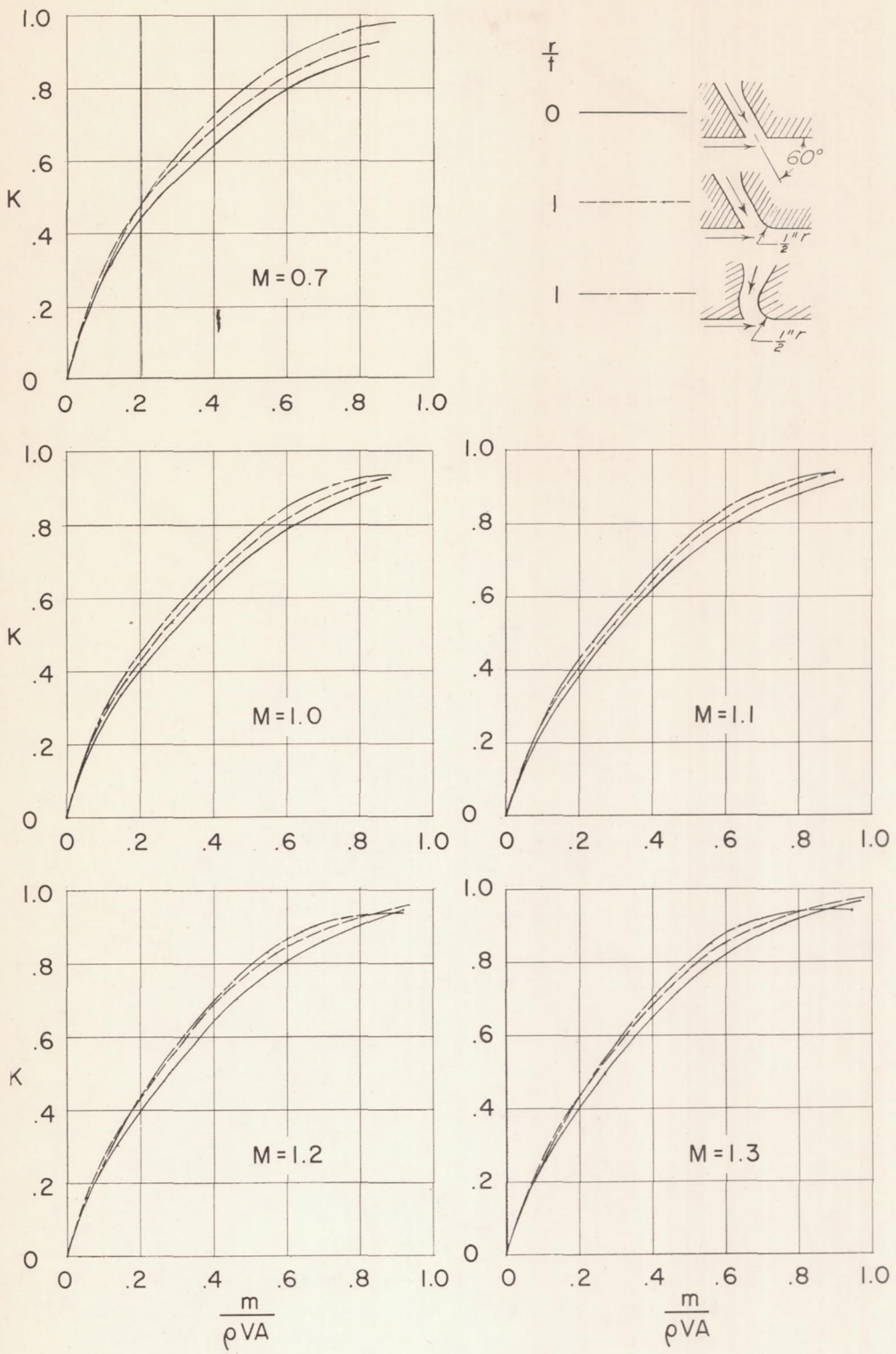

Figure 16.- Comparison of discharge coefficients of curved outlet and 60° outlets.

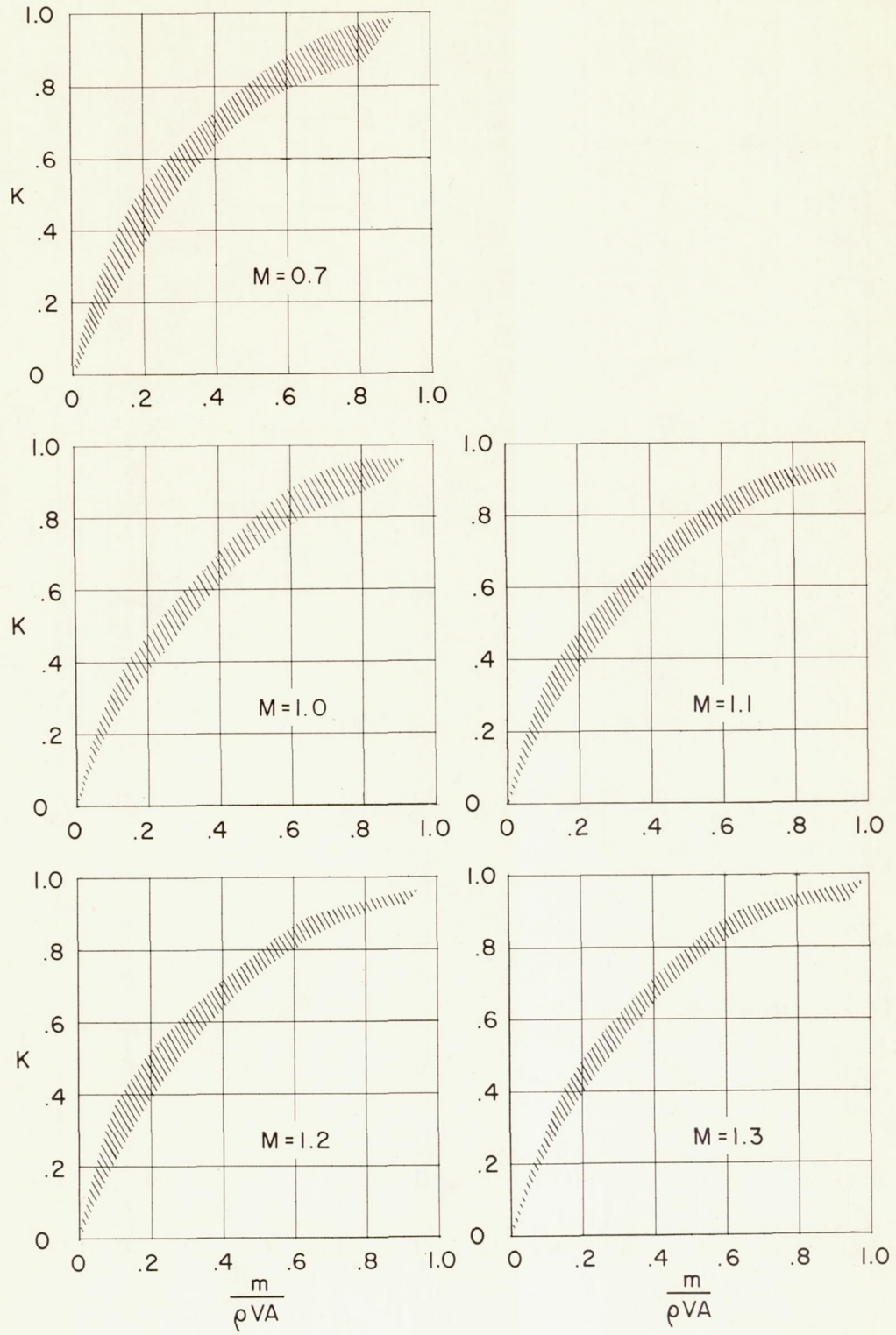

Figure 17.- Range of discharge coefficient as a function of discharge flow ratio for all flush ducted outlets.

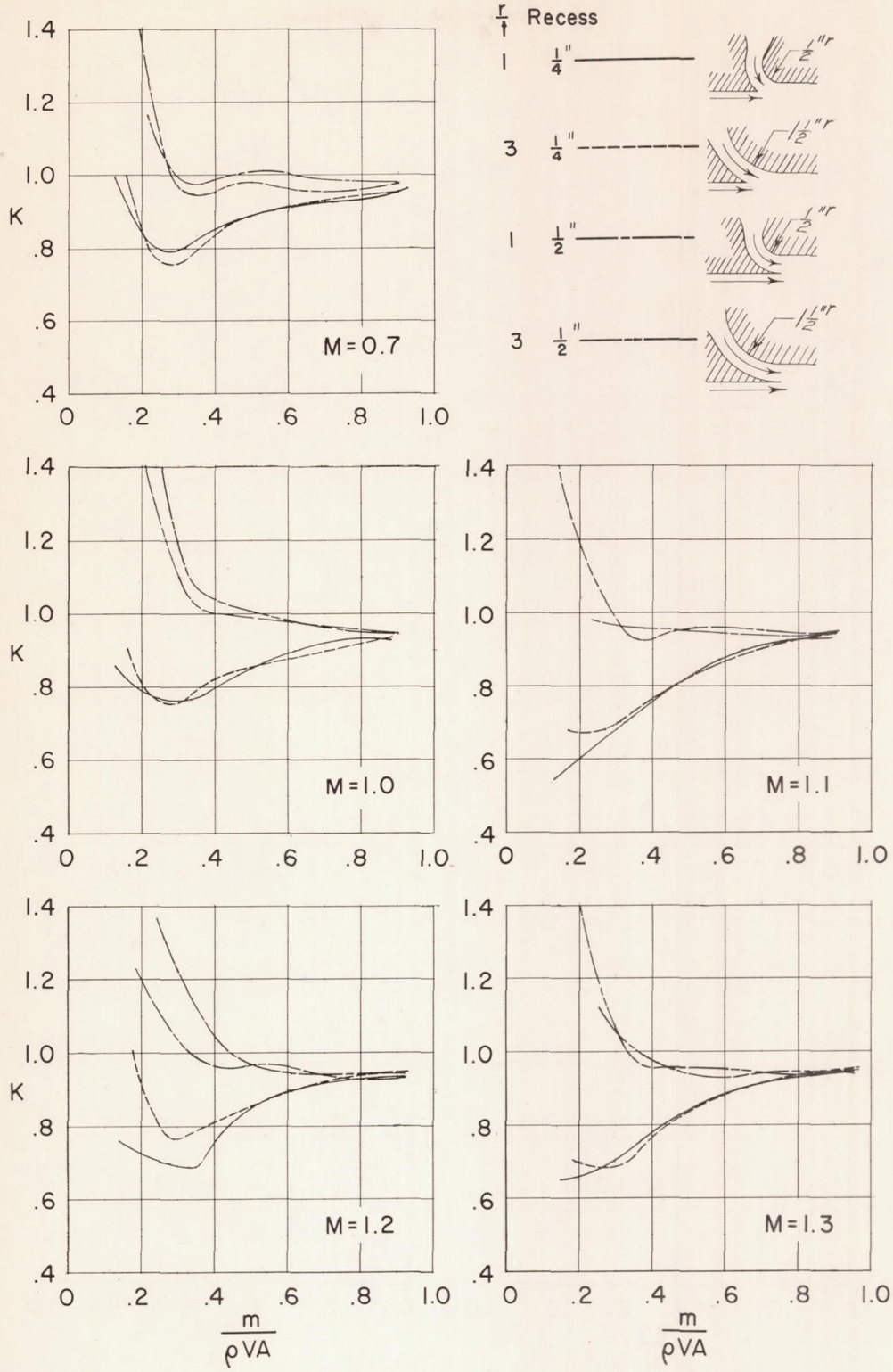

Figure 18.- Discharge coefficient as a function of discharge flow ratio for recessed outlets.

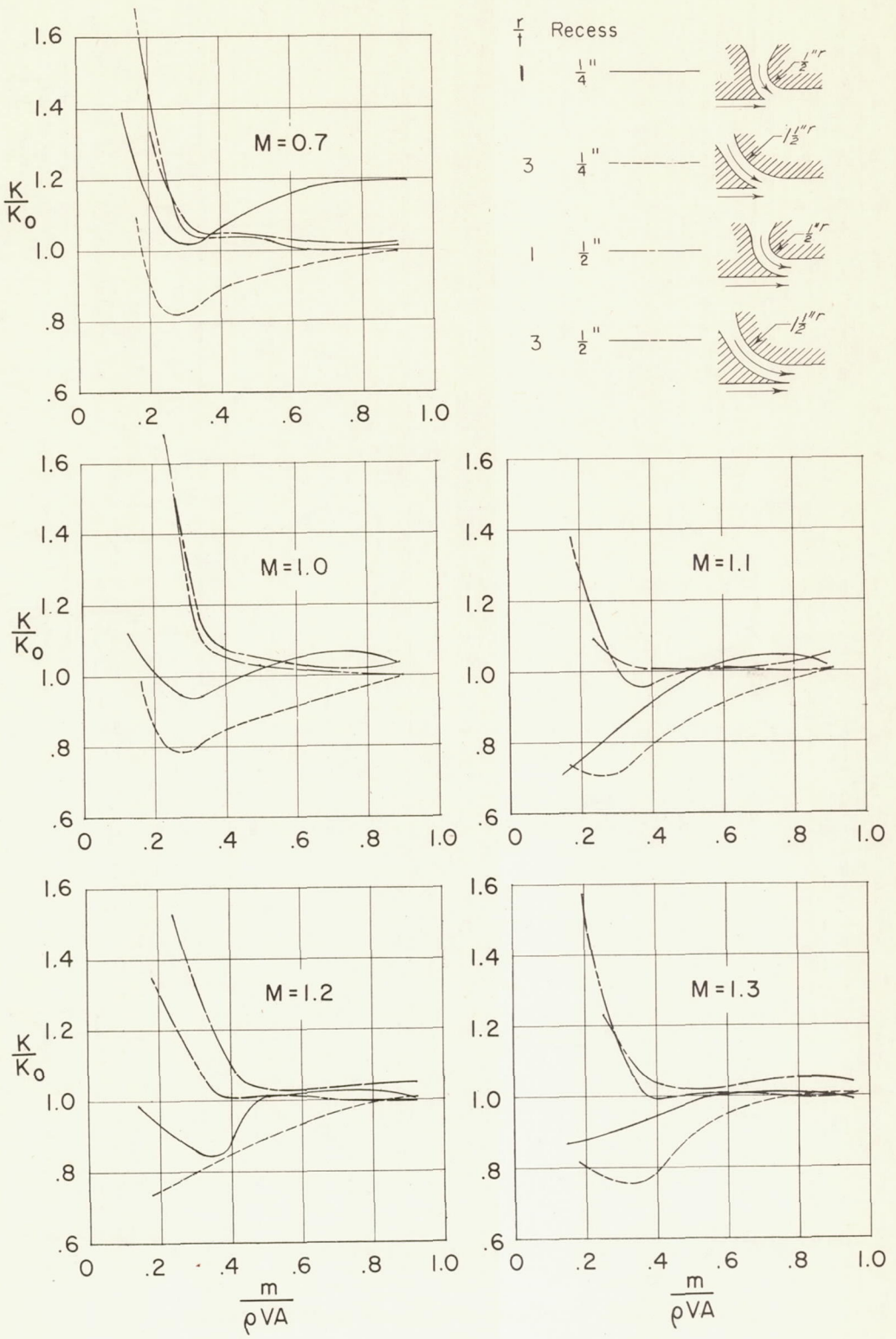

Figure 19.- Ratio of discharge coefficient to free-jet coefficient as a function of discharge flow ratio for recessed outlets.

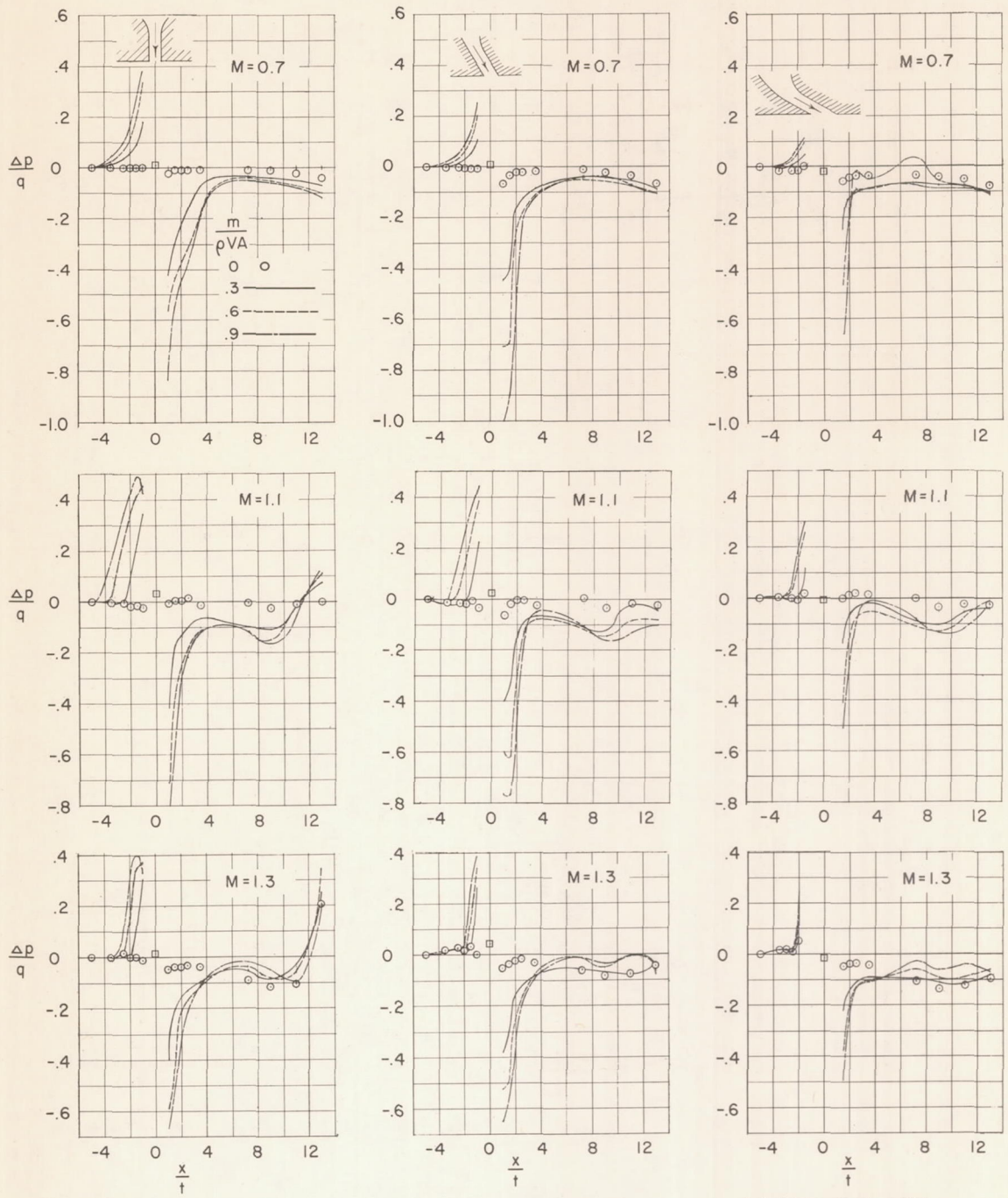

(a) 90° inclined outlet.

(b) 60° inclined outlet.

(c) 30° inclined outlet.

Figure 20.- Surface pressure distributions.

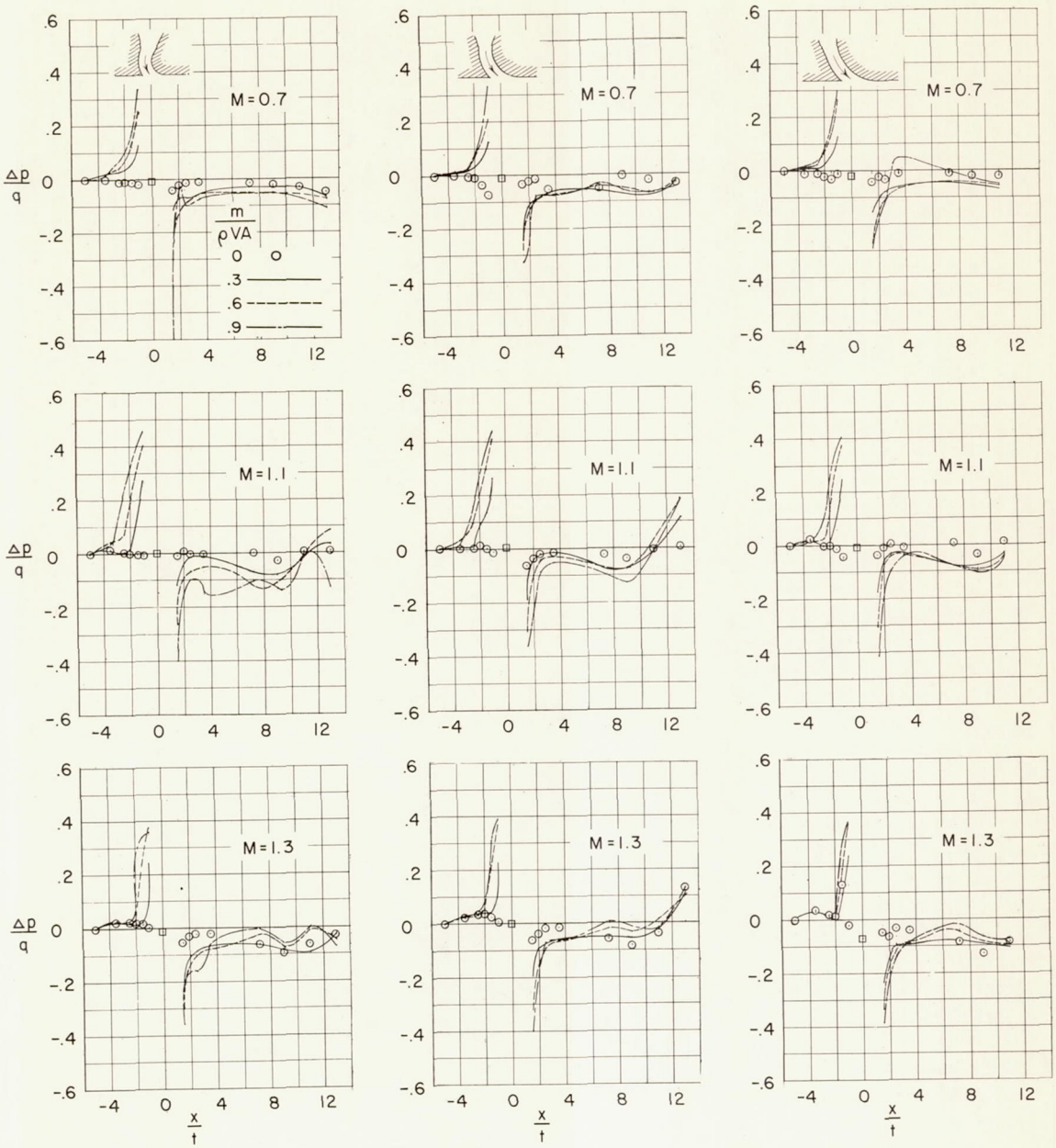

Figure 20.- Continued.

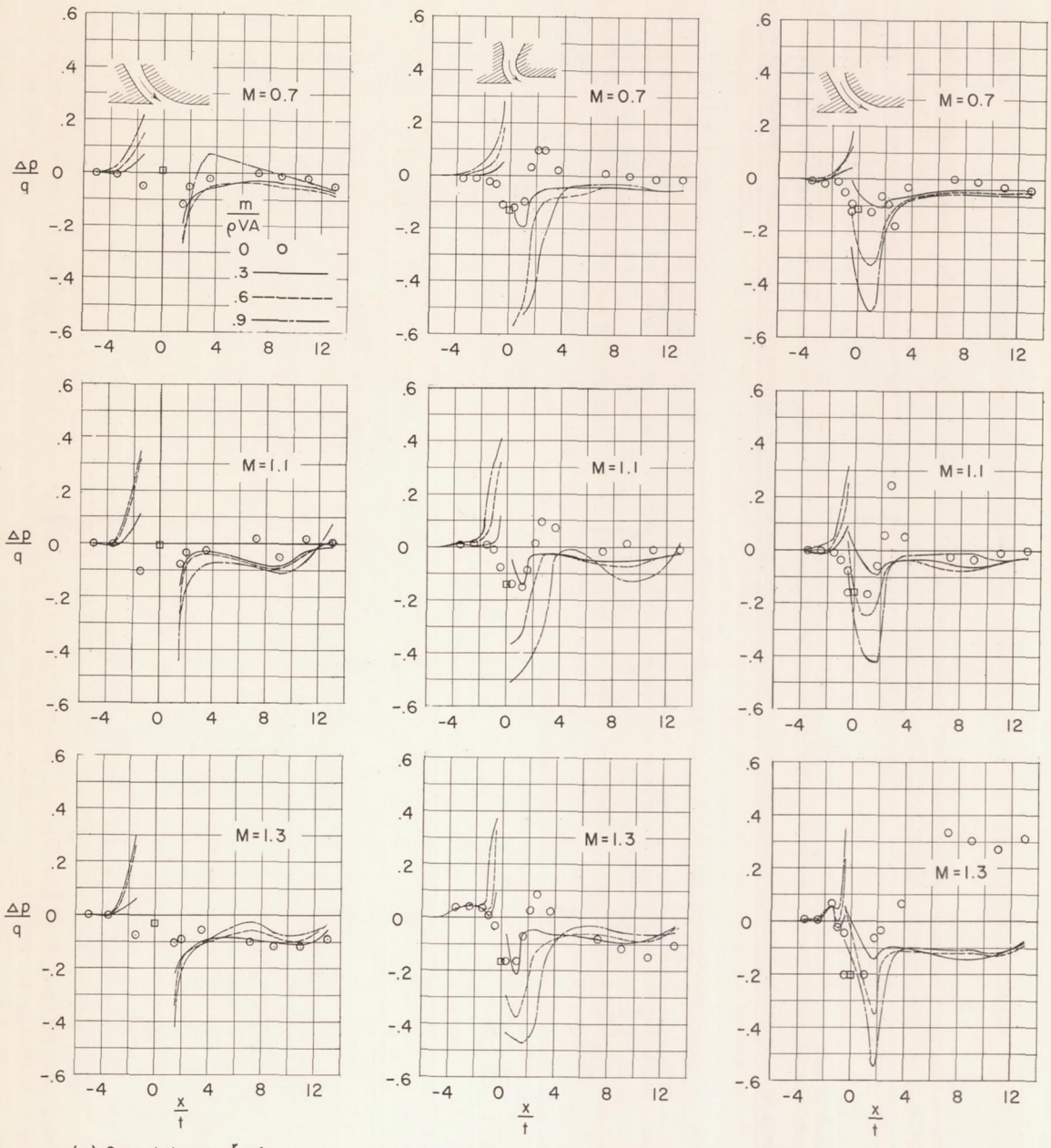

(g) Curved throat, $\frac{r}{t} = 4$.

(h) Shallow recessed outlet, $\frac{r}{t} = 1$.

(i) Shallow recessed outlet, $\frac{r}{t} = 3$.

Figure 20.- Continued.

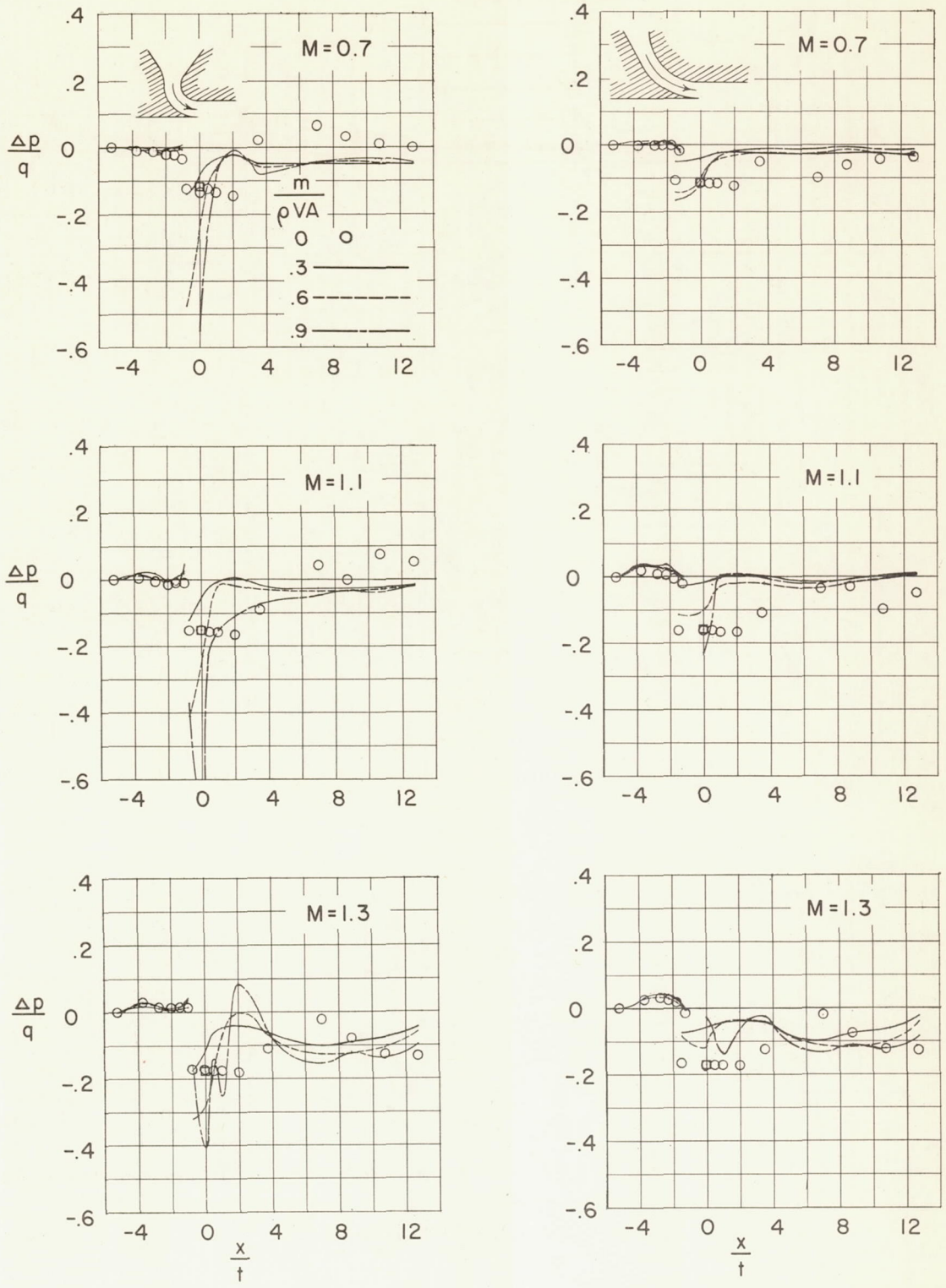

(j) Deep recessed outlet, $\frac{r}{t} = 1.$

(k) Deep recessed outlet, $\frac{r}{t} = 3.$

Figure 20.- Concluded.

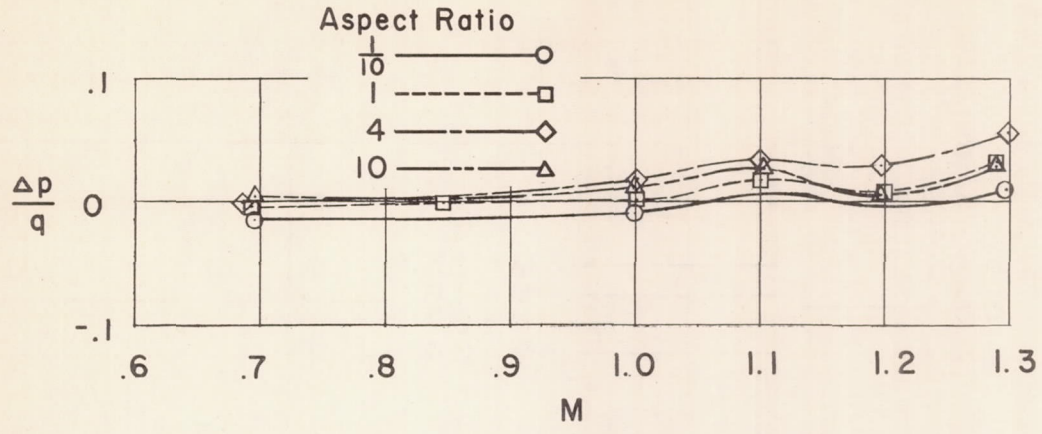

Thin-plate Outlets

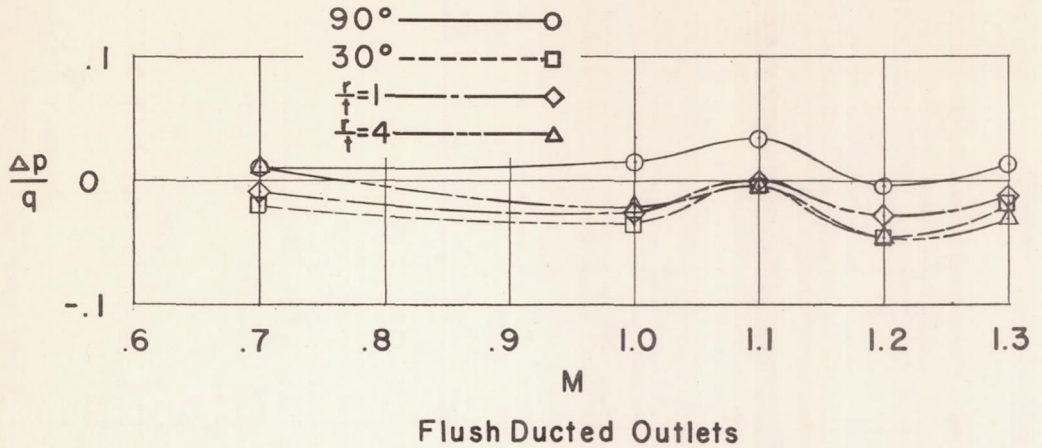

Flush Ducted Outlets

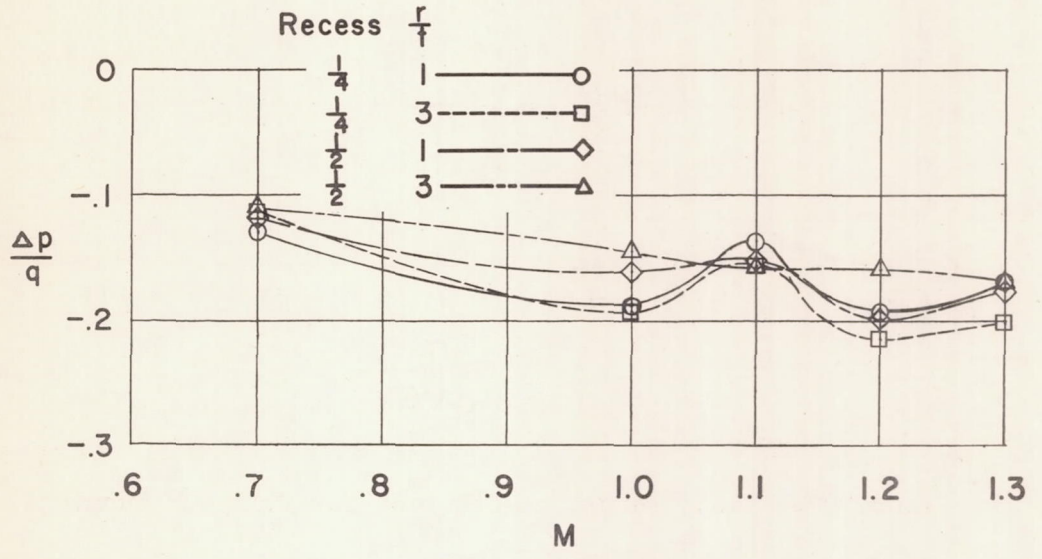

Recessed Outlets

Figure 21.- Vent pressures.

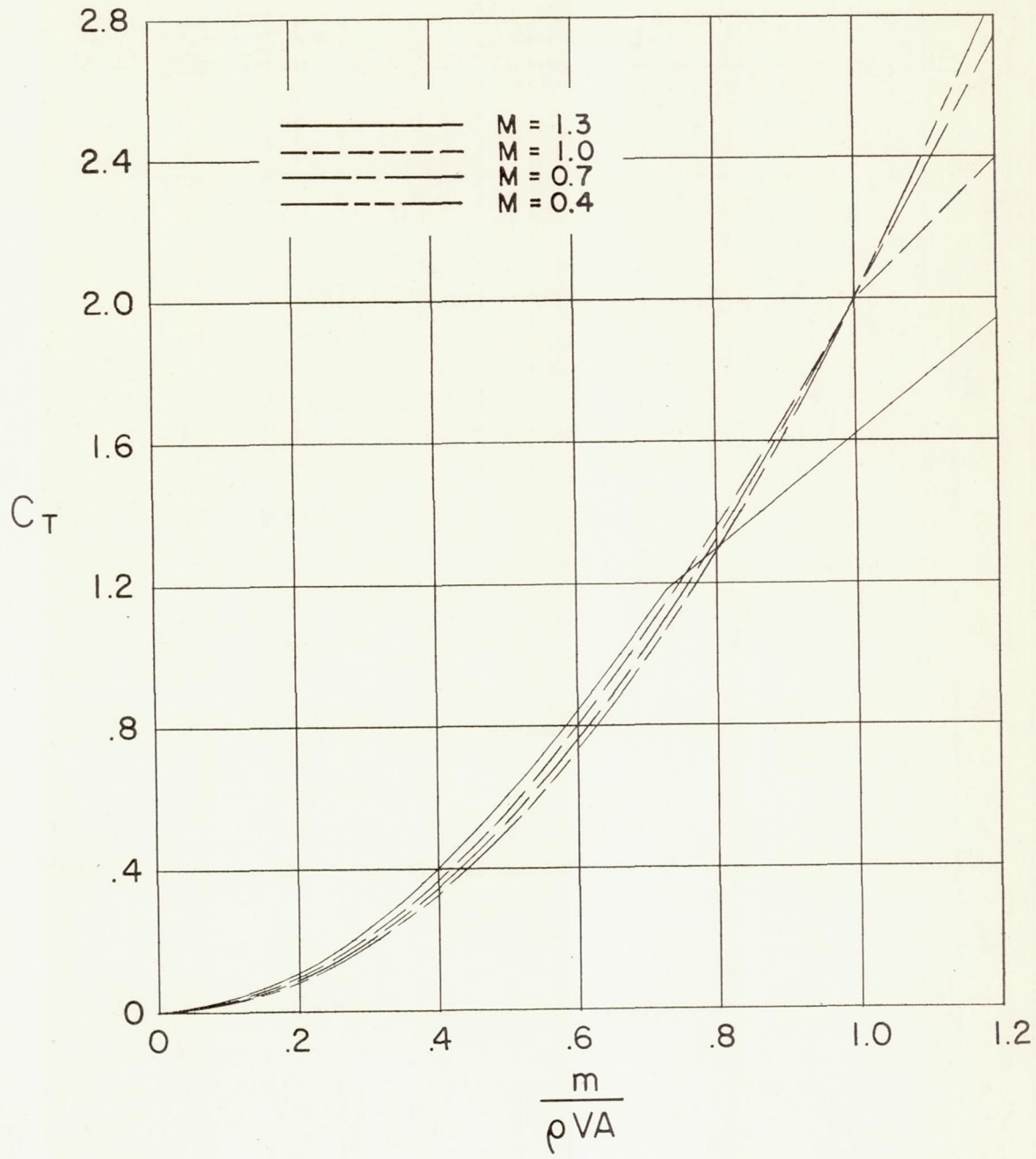

Figure 22.- Ideal thrust coefficient for full 90° turning.

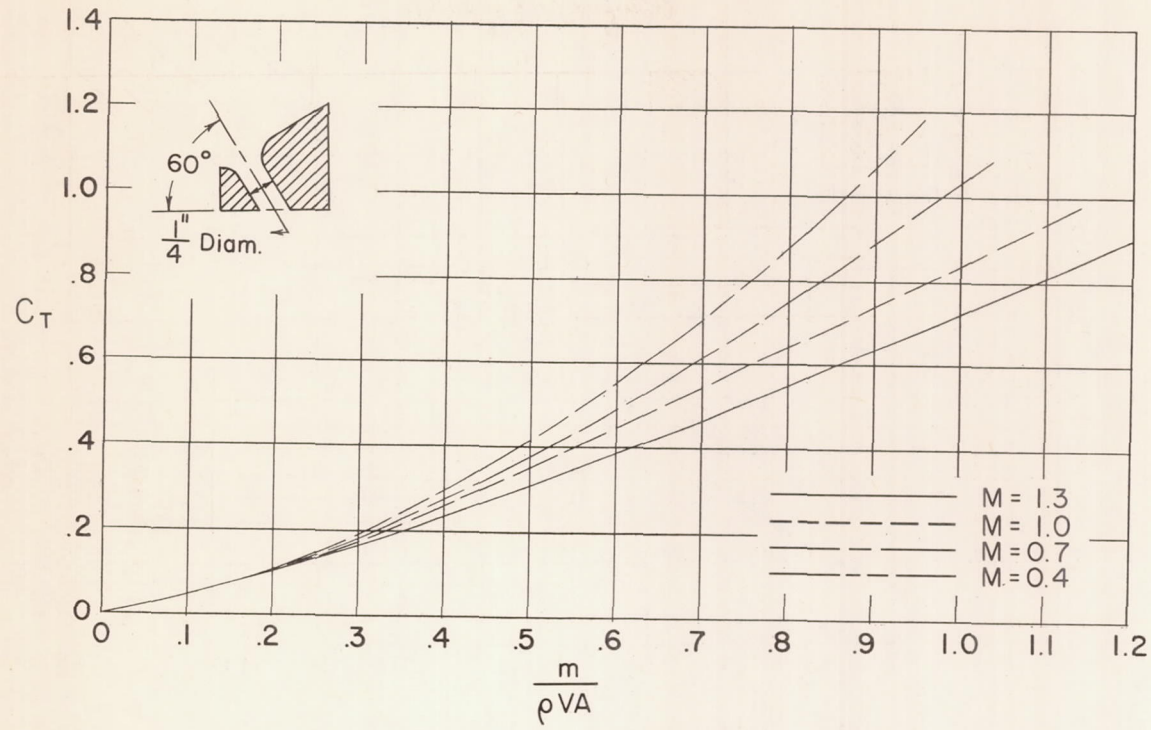

(a) 60° Inclined ducted outlet.

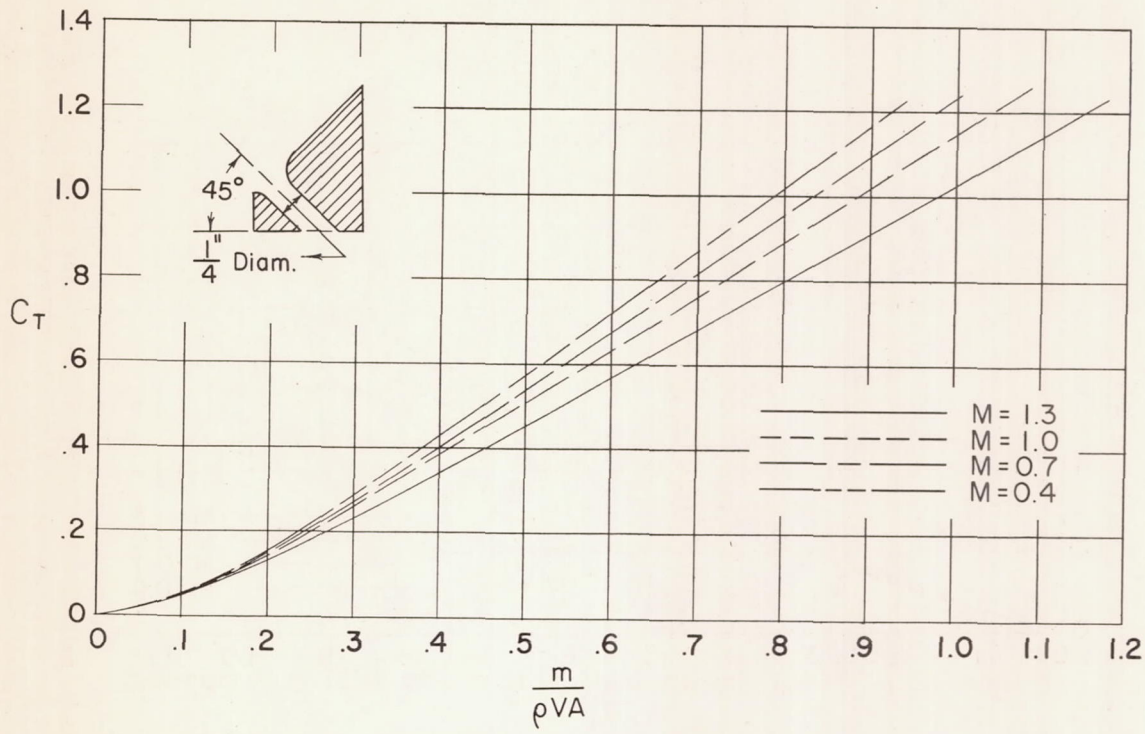

(b) 45° Inclined ducted outlet.

Figure 23.- Thrust coefficients for circular ducted outlets with various angles of inclination.

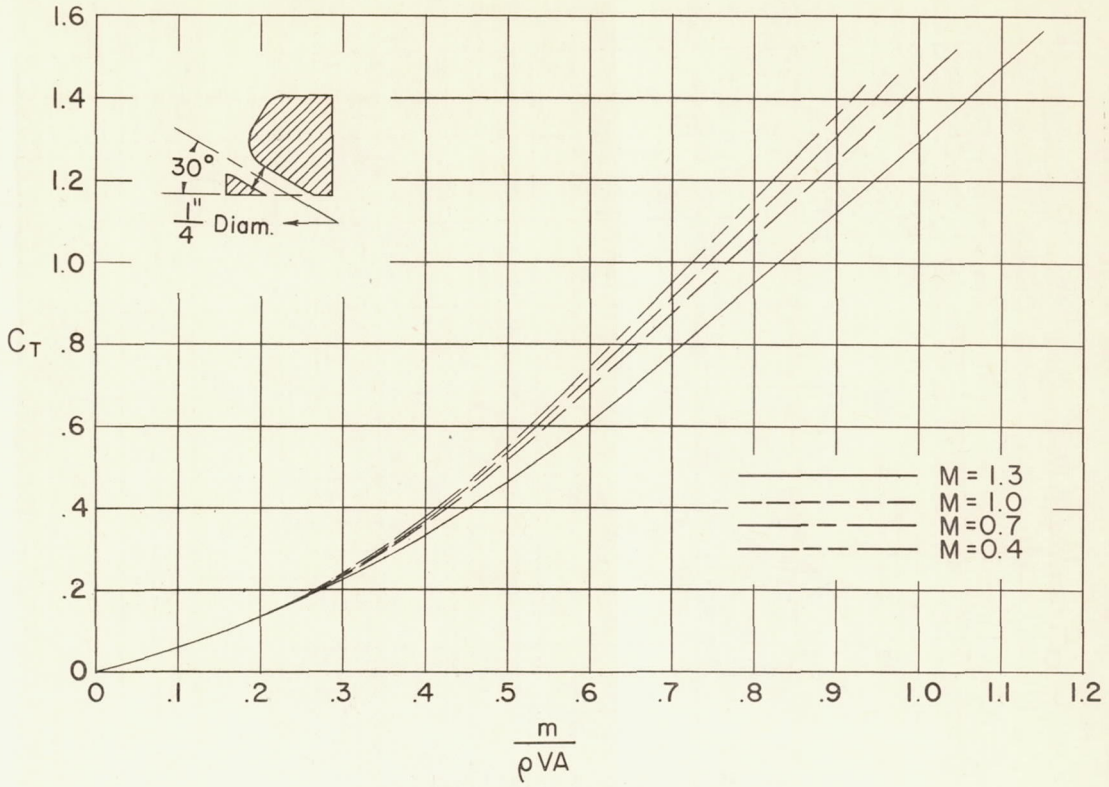

(c) 30° inclined ducted outlet.

Figure 23.- Concluded.

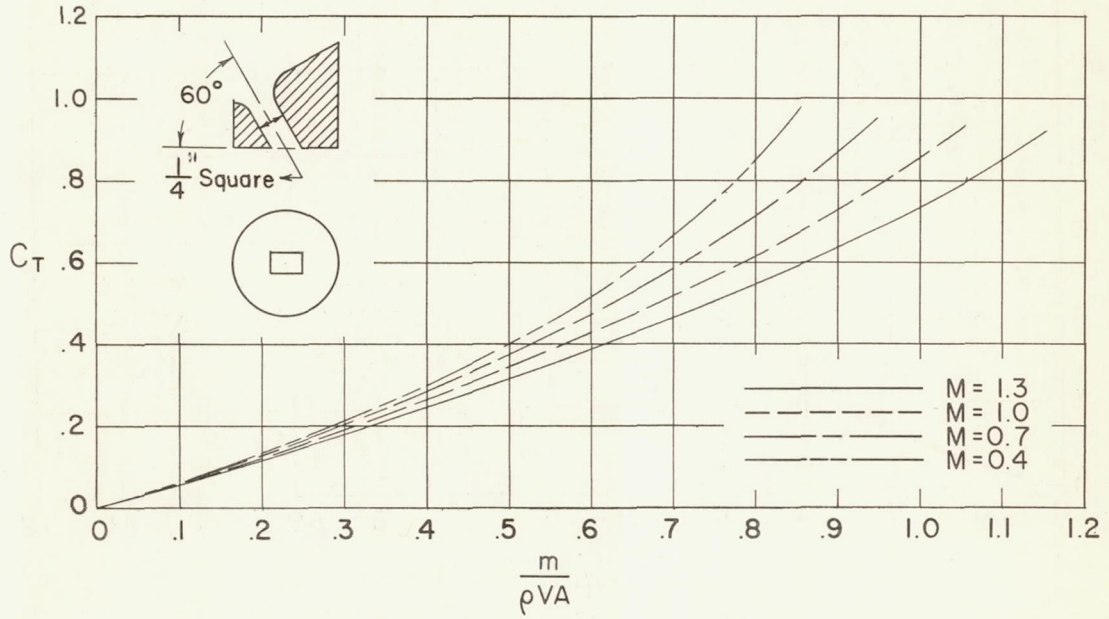

Figure 24.- Thrust coefficients for a square 60° inclined ducted outlet.